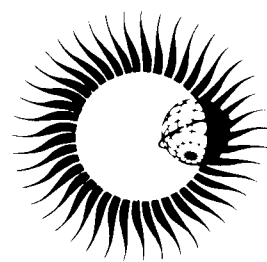


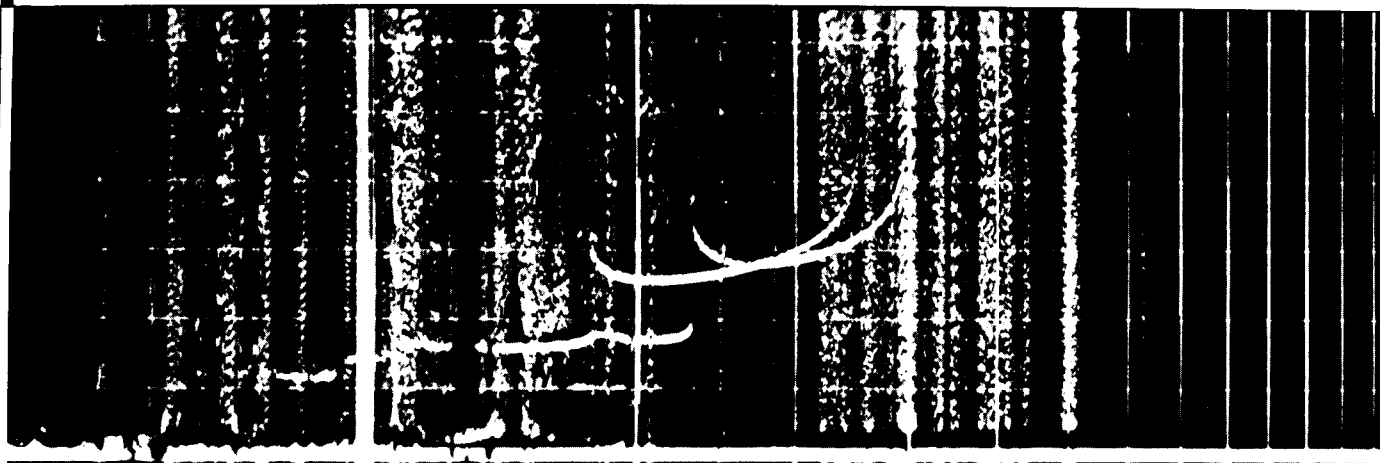
WORLD DATA CENTER A  
for  
Solar-Terrestrial Physics



IONOGRAM ANALYSIS  
WITH THE GENERALISED PROGRAM POLAN



December 1985



WORLD DATA CENTER A  
National Academy of Sciences  
2101 Constitution Avenue, NW  
Washington, D.C. 20418 USA

-----  
World Data Center A consists of the Coordination Office  
and the following eight Subcenters:

COORDINATION OFFICE  
World Data Center A  
National Academy of Sciences  
2101 Constitution Avenue, NW  
Washington, D.C. 20418 USA  
[Telephone: (202) 334-3359]

GLACIOLOGY (Snow and Ice)  
World Data Center A: Glaciology  
(Snow and Ice)  
Cooperative Inst. for Research in  
Environmental Sciences  
University of Colorado  
Boulder, Colorado 80309 USA  
Telephone: (303) 492-5171

MARINE GEOLOGY AND GEOPHYSICS  
(Gravity, Magnetics, Bathymetry,  
Seismic Profiles, Marine Sediment,  
and Rock Analyses):

World Data Center A for Marine  
Geology and Geophysics  
NOAA, E/GC3  
325 Broadway  
Boulder, Colorado 80303 USA  
Telephone: (303) 497-6487

METEOROLOGY (and Nuclear Radiation)  
World Data Center A: Meteorology  
National Climatic Data Center  
NOAA, E/CC  
Federal Building  
Asheville, North Carolina 28801 USA  
Telephone: (704) 259-0682

OCEANOGRAPHY  
World Data Center A: Oceanography  
National Oceanographic Data Center  
NOAA, E/OC  
2001 Wisconsin Avenue, NW  
Page Bldg. 1, Rm. 414  
Washington, D.C. 20235 USA  
Telephone: (202) 634-7510

ROCKETS AND SATELLITES  
World Data Center A: Rockets and  
Satellites  
Goddard Space Flight Center  
Code 601  
Greenbelt, Maryland 20771 USA  
Telephone: (301) 344-6695

ROTATION OF THE EARTH  
World Data Center A: Rotation  
of the Earth  
U.S. Naval Observatory  
Washington, D.C. 20390 USA  
Telephone: (202) 653-1507

SOLAR-TERRESTRIAL PHYSICS (Solar and  
Interplanetary Phenomena, Ionospheric  
Phenomena, Flare-Associated Events,  
Geomagnetic Variations, Aurora,  
Cosmic Rays, Airglow):

World Data Center A  
for Solar-Terrestrial Physics  
NOAA, E/GC2  
325 Broadway  
Boulder, Colorado 80303 USA  
Telephone: (303) 497-6323

SOLID-EARTH GEOPHYSICS (Seismology,  
Tsunamis, Gravimetry, Earth Tides,  
Recent Movements of the Earth's  
Crust, Magnetic Measurements,  
Paleomagnetism and Archeomagnetism,  
Volcanology, Geothermics):

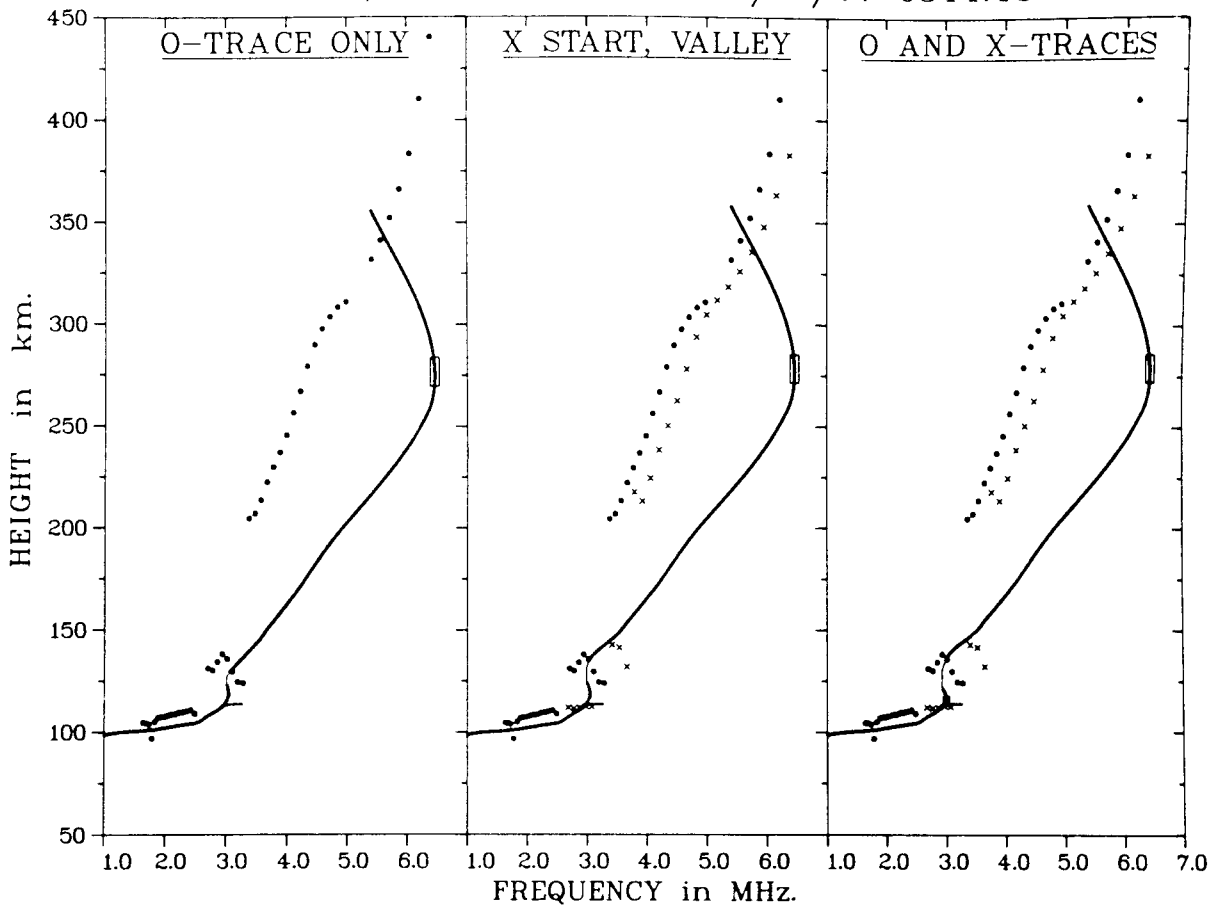
World Data Center A  
for Solid-Earth Geophysics  
NOAA, E/GC1  
325 Broadway  
Boulder, Colorado 80303 USA  
Telephone: (303) 497-6521

World Data Centers conduct international exchange of geophysical observations in accordance with the principles set forth by the International Council of Scientific Unions. WDC-A is established in the United States under the auspices of the National Academy of Sciences. Communications regarding data interchange matters in general and World Data Center A as a whole should be addressed to World Data Center A, Coordination Office (see address above). Inquiries and communications concerning data in specific disciplines should be addressed to the appropriate subcenter listed above.

IONOGRAM ANALYSIS WITH THE GENERALISED PROGRAM POLAN

KAUAI, HAWAII

09/16/77 0844:43



Profiles calculated from digital data obtained with the NOAA Dynasonde.

The program used includes automatic identification and analysis of sporadic E traces. Error boxes at the layer peaks are based on the peak fitting errors returned by POLAN. The center curve is the normal analysis in which POLAN selects only those extraordinary ray data which are useful for start and valley calculations. The right hand curve uses all ordinary and extraordinary data -- this is not normally recommended since differences in echo occurrence, and horizontal separation of the rays, can produce a distorted profile.

Acknowledgements: Some of the work described in this report was carried out while the author was a guest worker at the NOAA Space Environment Laboratories, Boulder, Colorado. I am grateful to Dr. L. F. McNamara for his assistance in the final preparation of this report.

# WORLD DATA CENTER A for Solar-Terrestrial Physics



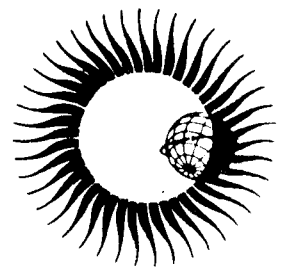
REPORT UAG-93

## IONOGRAM ANALYSIS WITH THE GENERALISED PROGRAM POLAN

by

J.E. TITHERIDGE  
Physics Department  
The University of Auckland  
Private Bag, Auckland,  
New Zealand

December 1985



U.S. DEPARTMENT OF COMMERCE  
NATIONAL OCEANIC AND ATMOSPHERIC ADMINISTRATION  
NATIONAL ENVIRONMENTAL SATELLITE, DATA, AND INFORMATION SERVICE  
National Geophysical Data Center  
Boulder, CO 80303 USA

## DESCRIPTION OF WORLD DATA CENTERS

World Data Centers conduct international exchange of geophysical observations in accordance with the principles set forth by the International Council of Scientific Unions (ICSU). They were established in 1957 by the International Geophysical Year Committee (CSAGI) as part of the fundamental international planning for the IGY program to collect data from the numerous and widespread IGY observational programs and to make such data readily accessible to interested scientists and scholars for an indefinite period of time. WDC-A was established in the U.S.A.; WDC-B, in the U.S.S.R.; and WDC-C, in Western Europe, Australia, and Japan. This new system for exchanging geophysical data was found to be very effective, and the operations of the World Data Centers were extended by ICSU on a continuing basis to other international programs; the WDC's were under the supervision of the Comité International de Géophysique (CIG) for the period 1960 to 1967 and are now supervised by the ICSU Panel on World Data Centres.

The current plans for continued international exchange of geophysical data through the World Data Centers are set forth in the *Fourth Consolidated Guide to International Data Exchange through the World Data Centres*, issued by the ICSU Panel on World Data Centres. These plans are broadly similar to those adopted under ICSU auspices for the IGY and subsequent international programs.

### Functions and Responsibilities of WDC's

The World Data Centers collect data and publications for the following disciplines: Glaciology; Meteorology; Oceanography; Rockets and Satellites; Solar-Terrestrial Physics disciplines (Solar and Interplanetary Phenomena, Ionospheric Phenomena, Flare Associated Events, Geomagnetic Phenomena, Aurora, Cosmic Rays, Airglow); Solid-Earth Geophysics disciplines (Seismology, Tsunamis, Marine Geology and Geophysics, Gravimetry, Earth Tides, Recent Movements of the Earth's Crust, Rotation of the Earth, Magnetic Measurements, Paleomagnetism and Archeomagnetism, Volcanology, Geothermics). In planning for the various scientific programs, decisions on data exchange were made by the scientific community through the international scientific unions and committees. In each discipline the specialists themselves determined the nature and form of data exchange, based on their needs as research workers. Thus the type and amount of data in the WDC's differ from discipline to discipline.

The objects of establishing several World Data Centers for collecting observational data were: (1) to insure against loss of data by the catastrophic destruction of a single center, (2) to meet the geographical convenience of, and provide easy communication for, workers in different parts of the world. Each WDC is responsible for: (1) endeavoring to collect a complete set of data in the field or discipline for which it is responsible, (2) safe-keeping of the incoming data, (3) correct copying and reproduction of data, maintaining adequate standards of clarity and durability, (4) supplying copies to other WDC's of data not received directly, (5) preparation of catalogs of all data in its charge, and (6) making data in the WDC's available to the scientific community. The WDC's conduct their operation at no expense to ICSU or to the ICSU family of unions and committees.

### World Data Center A

World Data Center A, for which the National Academy of Sciences through the Geophysics Research Board and its Committee on Data Interchange and Data Centers has over-all responsibility, consists of the WDC-A Coordination Office and seven subcenters at scientific institutions in various parts of the United States. The GRB periodically reviews the activities of WDC-A and has conducted several studies on the effectiveness of the WDC system. As a result of these reviews and studies some of the subcenters of WDC-A have been relocated so that they could more effectively serve the scientific community. The addresses of the WDC-A subcenters and Coordination Office are given inside the front cover.

The data received by WDC-A have been made available to the scientific community in various ways: (1) reports containing data and results of experiments have been compiled, published, and widely distributed; (2) synoptic type data on cards, microfilm, or tables are available for use at the subcenters and for loan to scientists; (3) copies of data and reports are provided upon request.

## TABLE OF CONTENTS

|   | <u>Page</u> |
|---|-------------|
| Frontispiece and acknowledgements                               |             |
| ABSTRACT . . . . .  | 1           |
| LIST OF FIGURES AND TABLES . . . . .                            | 2           |
| TERMINOLOGY . . . . .   | 4           |
| <b>1. INTRODUCTION . . . . .</b>                                | <b>6</b>    |
| <b>2. IONOGRAM ANALYSIS PROCEDURES</b>                          |             |
| 2.1 Lamination Methods . . . . .                                | 8           |
| 2.2 Single Polynomial Methods . . . . .                         | 8           |
| 2.3 Overlapping Polynomials . . . . .                           | 9           |
| 2.4 Least-Squares Solutions . . . . .                           | 10          |
| <b>3. SELECTION OF AN <math>N(H)</math> METHOD</b>              |             |
| 3.1 Rapid Estimation of Layer Constants . . . . .               | 11          |
| 3.2 Calculation of Monotonic Profiles . . . . .                 | 11          |
| 3.3 Full Calculations . . . . .                                 | 12          |
| <b>4. A GENERALISED FORMULATION</b>                             |             |
| 4.1 Outline . . . . .   | 13          |
| 4.2 The Basic Equations . . . . .                               | 13          |
| 4.3 Calculation Procedures . . . . .                            | 15          |
| <b>5. THE PROGRAM POLAN</b>                                     |             |
| 5.1 General Characteristics . . . . .                           | 16          |
| 5.2 The Standard Modes of Analysis . . . . .                    | 17          |
| 5.3 Curve Fitting Procedures . . . . .                          | 19          |
| 5.4 The Layer Peak . . . . .                                    | 21          |
| 5.5 The Simplified Program SPOLAN . . . . .                     | 22          |
| <b>6. STARTING PROCEDURES FOR THE ORDINARY RAY</b>              |             |
| 6.1 Outline . . . . .   | 23          |
| 6.2 The Methods Used in POLAN . . . . .                         | 24          |
| 6.3 Daytime Starting Models . . . . .                           | 25          |
| 6.4 A Night-time Starting Model . . . . .                       | 27          |
| <b>7. VALLEY PROCEDURES FOR THE ORDINARY RAY</b>                |             |
| 7.1 Outline . . . . .   | 28          |
| 7.2 The Standard Valley . . . . .                               | 28          |
| 7.3 Addition of Physical Constraints . . . . .                  | 30          |
| 7.4 Valley Options in POLAN . . . . .                           | 33          |
| <b>8. START CALCULATIONS USING THE EXTRAORDINARY RAY</b>        |             |
| 8.1 Practically Obtainable Information . . . . .                | 36          |
| 8.2 Inclusion of Extraordinary-Ray Data . . . . .               | 37          |
| 8.3 The Slab Start in POLAN . . . . .                           | 39          |
| 8.4 Physical Constraints and Height Iteration . . . . .         | 41          |
| 8.5 The Choice of Scaling Frequencies . . . . .                 | 45          |
| 8.6 Other Start Procedures . . . . .                            | 49          |
| <b>9. VALLEY CALCULATIONS USING THE EXTRAORDINARY RAY</b>       |             |
| 9.1 Introduction . . . . .                                      | 53          |
| 9.2 The Normal Analysis - Calculation of Valley Width . . . . . | 54          |
| 9.3 Calculation of Valley Width and Depth . . . . .             | 56          |
| 9.4 Results With Test Model Ionograms . . . . .                 | 58          |

|  |     |
|--|-----|
| <b>10. USING POLAN</b>   |     |
| 10.1 Implementation . . . . .  | 63  |
| 10.2 POLAN Input Data . . . . .  | 64  |
| 10.3 POLAN Output Data . . . . .   | 67  |
| 10.4 Selection and Scaling of Data . . . . .   | 69  |
| 10.5 Selection of a Value for START . . . . .  | 73  |
| <b>11. SCALING AND ANALYSIS WITH THE PROGRAM SCION</b>                               |     |
| 11.1 Outline . . . . .   | 74  |
| 11.2 Entering Initial Specifications . . . . .                                       | 75  |
| 11.3 Defining the Ionogram Coordinates . . . . .                                     | 75  |
| 11.4 Scaling the Ordinary-Ray Trace . . . . .  | 77  |
| <b>REFERENCES</b> . . . . .  | 79  |
| <b>APPENDIX A. THE ABSOLUTE ACCURACY OF THE CALCULATED PROFILES</b>                  |     |
| A.1 Relative accuracies with smooth virtual height curves . . . . .                  | 81  |
| A.2 The analysis of irregular profiles . . . . .                                     | 83  |
| A.3 The effect of errors in the virtual height data . . . . .                        | 85  |
| <b>APPENDIX B. DEPENDENCE OF THE GROUP REFRACTIVE INDEX ON DIP ANGLE</b>             |     |
| B.1 Values of group index . . . . .  | 88  |
| B.2 Information obtainable using O and X rays . . . . .                              | 91  |
| B.3 The reduction of integration errors at high dip angles . . . . .                 | 93  |
| <b>APPENDIX C. THE EFFECTS OF A VARYING GYROFREQUENCY</b>                            |     |
| C.1 Values of gyrofrequency in the ionosphere . . . . .                              | 96  |
| C.2 Changes near reflection . . . . .  | 97  |
| C.3 Retardation in the underlying region . . . . .                                   | 99  |
| C.4 Model studies . . . . .  | 102 |
| C.5 The choice of gyrofrequency for the underlying regions . . . . .                 | 104 |
| <b>APPENDIX D. GROUP INDEX CALCULATIONS WITHIN POLAN</b>                             |     |
| D.1 Calculation of the virtual height coefficients - The subroutine COEFIC . . . . . | 108 |
| D.2 Delay in the underlying ionisation - The subroutine REDUCE . . . . .             | 111 |
| D.3 Calculation of the group refractive index - The subroutine GIND . . . . .        | 114 |
| <b>APPENDIX E. THE CONSTRUCTION OF POLAN</b>   |     |
| E.1 Logic Flow . . . . .   | 116 |
| E.2 Start and Valley Procedures . . . . .  | 122 |
| E.3 Program Parameters . . . . .   | 125 |
| <b>APPENDIX F. PROGRAM LISTINGS</b>  |     |
| F.1 The main subroutine POLAN . . . . .  | 128 |
| F.2 The subroutines SETUP, SELDAT and STAVAL . . . . .                               | 134 |
| F.3 The subroutines COEFIC, ADJUST and REDUCE . . . . .                              | 141 |
| F.4 The subroutines PEAK, TRACE, SOLVE, SUMVAL and GIND . . . . .                    | 148 |
| F.5 The program SCION . . . . .  | 154 |
| <b>APPENDIX G. STANDARD TEST DATA AND RESULTS</b>                                    |     |
| G.1 The mainline program POLRUN . . . . .  | 161 |
| G.2 Standard test data . . . . .   | 163 |
| G.3 Standard results and discussion . . . . .  | 167 |
| <b>APPENDIX H. THE SIMPLIFIED PROGRAM SPOLAN</b>                                     |     |
| H.1 Construction . . . . .   | 178 |
| H.2 Test Results . . . . .   | 179 |
| H.3 Listings . . . . .   | 183 |



# IONOGRAM ANALYSIS WITH THE GENERALISED PROGRAM POLAN

by

J. E. TITHERIDGE

Physics Department, The University of Auckland  
Auckland, New Zealand

**ABSTRACT.** Different methods for the real-height analysis of ionograms, and their fields of application, are surveyed. A flexible new procedure is developed to give maximum accuracy and reliability in an automatic, one-pass analysis. The program POLAN uses polynomial real-height sections of any required degree, fitting any number of data points. By choice of a single parameter (MODE) it can reproduce all current methods from linear-laminations to single or overlapping polynomials. In addition a wide range of least-squares modes are available; these are preferable for most purposes, particularly with oversampled data (as from digital ionosondes). The mode of analysis changes automatically within the program to give an optimised least-squares calculation in the start, peak and valley regions. Physically unacceptable solutions are adjusted by imposing limits on the profile parameters. The new profile coefficients (and the new fitting error) are obtained directly and rapidly from the previous solution. This permits repeated application of the adjustments, as required, and cancellation of any change if it produces an unacceptably large increase in the virtual-height fitting error.

The information available using combined ordinary and extraordinary ray data is studied under different conditions. Procedures are developed which can solve the underlying and valley ambiguities with high accuracy, given suitable data, and which can detect and reject bad data. Physically reasonable models are incorporated into the least-squares start and valley calculations. This ensures an acceptable, standardised form for the profiles in these regions when only ordinary ray data are available. With good ordinary and extraordinary ray data POLAN produces the maximum amount of information which can be obtained about the unobserved regions, and results are almost independent of the physical models. With poor or inconsistent data, giving a less well-defined solution, results become increasingly biased towards the physical model so that acceptable results are obtained under most conditions.

Many of the techniques used in POLAN are new. Procedures and models developed for the start, peak and valley regions are described in reasonable detail, along with the precautions found to be necessary for maximum accuracy with extraordinary ray data. Mathematical procedures for ensuring full accuracy at all dip angles are described in the appendices. Optimum rules for scaling data are also developed and the practical use of POLAN is detailed. All programs are listed in the appendices, along with standard test data and the corresponding outputs. Copies of the programs are available on magnetic media from World Data Center A.

## SUMMARY LIST OF FIGURES AND TABLES

SECTIONS 1 TO 4 - No figures or tables.

### SECTION 5 - THE PROGRAM POLAN

|   |         |
|---|---------|
| TABLE 1. Parameters for the standard modes of analysis. | page 18 |
| FIGURE 1. The standard modes of analysis in POLAN.      | 18      |
| TABLE 2. Calculation times for each mode of POLAN.      | 20      |
| TABLE 3. Fitted heights and weights for each mode.      | 20      |

### SECTION 6 - START CALCULATIONS USING THE ORDINARY RAY

|  |    |
|--|----|
| FIGURE 2. The start extrapolation procedure using ordinary-ray data only.        | 23 |
| TABLE 4. Model starting heights for the analysis of daytime ionograms.           | 25 |
| FIGURE 3. Model starting frequencies (FN) for the analysis of daytime ionograms. | 26 |
| FIGURE 4. Model starting heights for the analysis of night-time ionograms.       | 27 |

### SECTION 7 - VALLEY CALCULATIONS USING THE ORDINARY RAY

|   |    |
|---|----|
| FIGURE 5. Possible real-height profiles corresponding to the same virtual height curve. | 29 |
| FIGURE 6. The form and notation of the standard valley.                                 | 29 |
| TABLE 5. Parameters for the standard valley.  | 29 |
| FIGURE 7. Profiles formed by the superposition of model Chapman layers.                 | 32 |
| FIGURE 8. Results from the analysis of dual Chapman-layer profiles.                     | 32 |
| FIGURE 9. Real-height changes due to a change in the assumed width of the E/F valley.   | 35 |

### SECTION 8 - START CALCULATIONS USING EXTRAORDINARY RAY DATA

|  |    |
|--|----|
| FIGURE 10. Parameters for the slab start profile used with extraordinary ray data.     | 40 |
| FIGURE 11. Slab start results at varying $f_{min}$ .                                   | 40 |
| TABLE 6. Results from the slab-start calculation of Figure 12.                         | 43 |
| FIGURE 12. Analysis of a difficult profile, with the addition of physical constraints. | 44 |
| FIGURE 13. Adjustments made by POLAN to compensate for bad data.                       | 44 |
| TABLE 7. Real height errors obtained using different scaling intervals.                | 47 |
| TABLE 8. Real height errors obtained with different values of $f_{min}$ .              | 48 |
| FIGURE 14. Virtual heights and gradients at low frequencies.                           | 48 |
| FIGURE 15. Polynomial start results, for different values of $f_{min}$ .               | 49 |
| TABLE 9. Real-height errors obtained with the polynomial start.                        | 50 |
| TABLE 10. The X-ray frequency shift used for starting corrections in SPOLAN.           | 51 |
| FIGURE 16. Results from the single-point starting correction in SPOLAN.                | 52 |

### SECTION 9 - VALLEY CALCULATIONS USING EXTRAORDINARY RAY DATA

|  |    |
|--|----|
| FIGURE 17. The shape of the standard valley model, for different values of VWIDTH. | 54 |
| FIGURE 18. Variations obtained by changing the depth of the model valley.          | 57 |
| FIGURE 19. Profiles used to investigate valley calculation procedures.             | 57 |

|   |  |     |
|---|--|-----|
| FIGURE 20.  | Results from 2-parameter valley calculations, at dip angles from 0 to 90°.   | 59  |
| FIGURE 21.  | Results at two different valley depths, for dip angles from 0 to 90°.        | 59  |
| FIGURE 22.  | Changes in real height and fitting error as the assumed valley depth varies. | 60  |
| FIGURE 23.  | The virtual-height fitting error as a function of assumed valley depth.      | 61  |
| <b>SECTION 10 - THE USE OF POLAN</b>                      |  |     |
| FIGURE 24.  | Scaling points for a typical daytime ionogram.                               | 71  |
| FIGURE 25.  | Regions where the 0-ray trace should not be scaled.                          | 71  |
| <b>SECTION 11 - THE PROGRAM SCION FOR DIGITISING DATA</b> |  |     |
| FIGURE 26.  | Ionogram layout for digitising, with "off-scale" areas.                      | 76  |
| <b>APPENDIX A - THE ACCURACY OF N(h) CALCULATIONS</b>     |  |     |
| TABLE A1.   | Real-height errors for a Chapman layer, with modes 1 to 7 of POLAN.          | 81  |
| TABLE A2.   | Real-height errors for a parabolic layer, for modes 1 to 7.                  | 82  |
| FIGURE A1.  | The real height profile used to produce a large cusp.                        | 83  |
| TABLE A3.   | Errors produced by a large cusp, for modes 1 to 6 of POLAN.                  | 84  |
| TABLE A4.   | Cusp errors obtained with different scaled frequency intervals.              | 85  |
| FIGURE A2.  | Changes in real height caused by changes in the starting correction.         | 87  |
| <b>APPENDIX B - DIP ANGLE VARIATIONS</b>                  |  |     |
| FIGURE B1.  | Relative group delays of the extraordinary and ordinary rays.                | 89  |
| FIGURE B2.  | The group delay ratio $R_{X,0}$ as a function of dip angle.                  | 89  |
| FIGURE B3.  | Polynomial fits to the 0- and X-ray group refractive indices.                | 90  |
| TABLE B1.   | Errors in the calculated real-height profile                                 | 92  |
| FIGURE B4.  | The effect of random errors in a slab start analysis.                        | 93  |
| FIGURE B5.  | Division of the group-index integration range, at high dip angles.           | 94  |
| FIGURE B6.  | Errors obtained with accurate virtual-height data at different dip angles.   | 95  |
| <b>APPENDIX C - FH HEIGHT VARIATION</b>                   |  |     |
| FIGURE C1.  | Measured values of gyrofrequency in the ionosphere.                          | 96  |
| TABLE C1.   | Changes in real and virtual height of a reflecting layer.                    | 98  |
| FIGURE C2.  | Changes in the X-ray virtual height due to a decrease in FH.                 | 99  |
| TABLE C2.   | The relative group retardation of 0 and X rays.                              | 100 |
| FIGURE C3.  | The equivalent monotonic distribution for an underlying layer.               | 101 |
| FIGURE C4.  | Virtual heights for a low layer and its equivalent monotonic distribution.   | 101 |
| TABLE C4.   | Errors in the slab start calculation, using fixed values of FH.              | 102 |
| FIGURE C5.  | Night E-region profiles used in developing rules for start calculations.     | 103 |
| FIGURE C6.  | Slab start calculations using a fixed value of gyrofrequency.                | 105 |
| FIGURE C7.  | Errors obtained from a model ionogram using different values of FH.          | 105 |
| FIGURE C8.  | The separation of "underlying" and "reflection" regions for FH.              | 106 |

## TERMINOLOGY

### 1. Physical Parameters.

I or DIP is the magnetic dip angle, in degrees.  
FB or FH is the electron gyrofrequency, in MHz.  
FB is the gyrofrequency at ground level, given in the call to POLAN. This is made negative if the gyrofrequency is to be height independent.  
FH is the current value of FB, corresponding to the height FHHT.  
FN = the plasma frequency in MHz.  
F = the wave frequency in MHz. Positive values are used for ordinary (O) ray data, and negative values for the extraordinary (X) ray.  
FR = the plasma frequency at reflection for the wave of frequency F. Thus  $FR = F$  for the O ray, and  $FR^2 = F(F + FH)$  for X rays (where F is negative).  
HR = the real height of reflection ( $h_j$ ) for the wave of frequency  $F_j$ .  
fmin = the lowest frequency in the given O-ray virtual-height data.  
h'min = the lowest virtual height for the ordinary ray. This may be at a frequency greater than fmin.  
G = the real-height gradient  $dh/dFN$ .  
T =  $(1 - FN^2/FR^2)^{.5}$ , varying from  $T = 1$  below the ionosphere to  $T = 0$  at the reflection height HR.  
 $\mu$  is the phase refractive index, varying from 1 at  $FN = 0$  to 0 at the height of reflection.  
 $\mu'$  is the group refractive index, varying from 1 at  $FN = 0$  to  $\sec(I)/T$  (for the O ray) at  $FN = FR$ .  
 $\chi$  is the solar zenith angle (Section 6.3).  
 $f_0, f_x$  are corresponding ordinary and extraordinary ray frequencies (reflected at the same value of plasma frequency).  
 $h'_0, h'_x$  are virtual heights for the ordinary and extraordinary rays.

### 2. Discrete Data Arrays.

$f_1, f_2, f_3, \dots, f_k, \dots$  (FC), (FCX) Scaled frequencies.  
 $h'_1, h'_2, h'_3, \dots, h'_k, \dots$  Scaled virtual heights.  
 $h_1, h_2, h_3, \dots, h_k, \dots$  HM Calculated real heights.  
FC, FCX are critical frequencies for the O and X rays respectively.  
k is the index of the current 'origin' ( $f_k, h_k$ ) to which the next step of the real height calculation is referenced. KR is used in place of k within POLAN.  
 $h''_n$  (where  $n > k$ ) is the 'reduced virtual height', equal to  $h'_n$  minus the group retardation due to those parts of the profile below the current origin ( $f_k, h_k$ ).  
FV, HT are the data arrays used in POLAN.  
Virtual-height data are initially moved up to start at FV(30), HT(30).  
Real-height data starts at FV(1), HT(1) and, as calculations progress, extends to overwrite the used virtual-heights.  
FA, HA is the origin for the current real-height polynomial.  
KR is the index of the current real-height origin, so that  $FA = FV(KR)$  and  $HA = HT(KR)$ .  
KV is the corresponding index into the virtual-height data, so that (normally)  
 $FV(KV) = FA$ , and  $HT(KV)$  is the reduced virtual height at the frequency FA.  
 $F_i, H_i, H'_i$  are discrete points within the range of the current real-height polynomial.  
i is a relative index, beginning at the current origin where  $FA = F_0, HA = H_0$ .  
Thus the polynomial calculation uses frequencies  $F_i = f_{k+i}$  for  $i = 1$  to MV.  
These correspond to frequencies FV(KR+1) to FV(KR+MV) in the given data array FV.  
 $H_i$  are the calculated real heights at the frequencies  $F_i$ .  
 $H'_i$  are the reduced virtual heights, equal to the scaled virtual heights  $h'_{k+i}$  less the group retardation in that section of the profile with plasma frequencies  $FN < F_0$ .

### 3. Profile Calculations.

The fitted real height expression is:

$$h - HA = \sum_{j=1}^{MT} q_j (FN - FA)^j \quad \text{giving real height } h \text{ as a function of plasma frequency } FN.$$

FA, HA define the origin of the current polynomial, i.e.  $FA = f_k = FV(KR)$  and  $HA = h_k = HT(KR)$ .  
 $q_j$  or  $q(j)$  are the polynomial coefficients for the current real height step.

AMODE is an input parameter specifying one of ten standard types of analysis, corresponding to different values of NT, NV, NR and NH (Section 5.2).

**The number of frequencies used:**

NV is the number of 0-ray virtual-height data points (above FA) to which the polynomial is to be fitted.  
NF is the number of 0-ray points actually used; normally equal to NV or to the number of 0-ray points available before a layer peak.  
NX is the number of X-ray data points used (in start and valley calculations). This is commonly equal to the number available in the range FA to FM + 0.1 MHz; points corresponding to  $FN > FM + 0.1$  MHz are deleted.  
MV = NX + NF is the total number of virtual heights fitted.  
FM = FV(MF) is the highest 0-ray frequency used in the current step.  
MF = KR + MV is the index corresponding to FM in the data arrays FV, HT.  
MX = KR + NX is the index of the highest X ray used.

**The number of terms used:**

NT is the initial number of terms to be used in the polynomial real height expression.  
MT is the number of polynomial terms actually used within POLAN. This is normally equal to  $NT + (NX+1)/2$ , with a maximum value of MV + NR.  
JM is the total number of real-height terms calculated, normally equal to MT. An additional term  $q(JM)$  [with  $JM = MT+1$ ] is included at a valley, or with an X-ray start calculation, to provide a calculated shift or offset  $h - HA = q(JM)$  in the height of the origin FA.  
NR is the number of known real heights above FA to be included in the polynomial fit (Section 5.2). If NR is negative, fitting is to 1 real height below FA and to  $|NR|-1$  heights above FA.  
NH is the number of new real heights to be calculated. This is equal to the number of points the origin is advanced for the next step.  $NH = 1$  for Modes 1 to 6, except just before a peak when  $NH = NF$  so that real heights are calculated at all fitted (0-ray) frequencies.

**4. Start, Peak and Valley Calculations.**

$f_s, h_s$  is the starting point for the profile calculation, with  $f_s \leq f_{min}$  and  $h_s \leq h'_{min}$ .  
 $f_s$  is normally 0.5 MHz, for an 0-ray calculation.

START is an input parameter specifying, normally, a model starting height ( $h_s$ ). Alternatively START may specify the value of  $f_s$  for a fixed starting height of 90, 110, 130, 150 or 170 km (Section 6.3). START = 0 gives an extrapolated value of  $h_s$ , while START = -1. sets  $f_s = f_{min}$  and  $h_s = h'_{min}$ .

FC is (i) a scaled 0-ray critical frequency,  
or (ii) the final calculated critical frequency of a layer peak.

FCX is a scaled X-ray critical frequency (Section 5.4).

SH is the calculated scale height of a (Chapman-layer) peak.

HMAX is the calculated peak height.

TCONT is the total electron content of the ionosphere up to the layer peak (including contributions from any lower layers).

HVAL is the virtual height corresponding to a critical frequency, and must be less than 30. If the given value  $h'(FC)$  is zero, HVAL is set equal to the parameter VALLEY in the call to POLAN.

VWIDTH is the overall width of the valley in km, equal to the height range over which the plasma frequency is less than the value FC for the underlying peak.

VDEPTH is the depth of a valley in MHz.

SHA is a model scale height for the neutral atmosphere, given by  $SHA = h/4 - 20$  km (Section 7.2). The 'standard valley' has a width of  $2.SHA = HMAX/2 - 40$  km, where HMAX is the height of the underlying peak.

VPEAK is the ratio (scale height above a peak)/(calculated scale height SH below the peak). VPEAK is currently set equal to 1.4, at the beginning of STAVAL, corresponding to a 40% increase in scale height above the peak.

PARHT is the height range for the initial parabolic section of the valley, extending from the layer peak to the valley bottom, with a scale height of 1.4 SH.

VBASE specifies the extent of the flat valley bottom, as a fraction of the distance (VWIDTH-PARHT) above the parabolic section. VBASE is currently set equal to 0.6. Above this flat section FN increases linearly from FV to FC, in a distance  $0.4(VWIDTH-PARHT)$ .

## 1. INTRODUCTION

The sweep-frequency ionosonde is a basic tool for ionospheric research. It produces records which can, in theory, be analysed to give the variation of electron density with height up to the peak of the ionosphere. Such electron-density profiles provide most of the information required for studies of the ionosphere and its effect on radio communications. Only a minute fraction of the recorded ionograms are analysed in this way, however, because of the effort required and the uncertain accuracy. To improve this situation we must make better use of the computing power now available, to reduce the need for manual selection of data and for careful appraisal of the results.

An ideal procedure for routine ionogram analysis should give consistently good results without operator intervention. This requires some built-in "intelligence" and adaptability. With high quality data we want the highest attainable accuracy. With normal data the procedure should have criteria for judging the acceptability of each individual point or profile parameter. It should be able to test, impose and remove physical constraints, and to smooth, de-weight, or reject bad data. Where a section of the profile cannot be calculated directly (such as the underlying, peak or valley regions) the procedure should use a defined physically-based model. Thus it should automatically do the "best" thing, in a consistent fashion, with widely varying types of data; if a normal best is not possible it should explain why and do the next-best.

The POLynomial ANalysis program POLAN is an attempt to meet some of these requirements. It provides an accurate and flexible procedure with adjustable resolution and the ability to mix physically desirable conditions with observed data in a weighted least-squares solution. The analysis can adapt readily to changes in the density and quality of data points, and respond in different ways to different situations. For routine work POLAN may be used as a "black box" with only the virtual height data, the magnetic dip angle and the gyrofrequency as required inputs. Optimised default procedures are then used in the analysis. If the input data is not self-consistent, and implies some physically unacceptable feature in the profile, this is noted and corrected. All results are obtained in a fully automatic, one-pass analysis.

POLAN is designed to reproduce current techniques (using linear laminations, parabolic laminations, single polynomials or fourth-order overlapping polynomials) by selection of a single parameter. It also provides a wide range of high order procedures, which are preferable for most work. When extraordinary ray data are not available, clearly defined and physically reasonable models are used for the start and valley regions. This allows direct comparison of results obtained under different conditions. When extraordinary ray data are available these are combined with the ordinary data in optimised procedures to resolve the starting and valley ambiguities. The physical models are included in the least-squares solutions for these regions, so that ill-defined data will give reasonable results (based primarily on the models). Peak parameters are determined by a least squares Chapman-layer fit to avoid the systematic scale height error inherent in a parabolic-peak approximation. Observed ordinary and extraordinary ray critical frequencies may be included in the peak calculation, to obtain best estimates of the critical frequency  $f_c$ , the probable error in  $f_c$ , the peak height and the scale height at the peak. With this careful combination of extraordinary ray data and physical constraints, POLAN is well suited to studies of the ionospheric scale height, the size of the valley between the E, F1 and F2 layers, and of ionisation below the night F layer.

A simplified version of POLAN, called SPOLAN, is described in appendix H. This reduces the extraordinary-ray calculations to a single-point starting correction. The layer peaks are parabolic, and some other refinements are omitted to give a much shorter and more understandable program. POLAN and SPOLAN are written as subroutines, so that a user may retain his own input and output data formats. The calling sequence, and the returned parameters, are the same for both programs.

Many new procedures are used in POLAN, to deal with problem areas in the  $N(h)$  calculation. These procedures are described in sufficient detail to give an understanding of the theory behind them, and the practical application. The main aims of this report are, however:-

- to offer some guidance in the selection of an appropriate method of ionogram analysis;
- to give an understanding of the general principles and approach used in POLAN;
- to provide the information required for effective use of POLAN; and
- to provide detailed documentation of the programs POLAN and SPOLAN so that they may be implemented with a minimum of frustration.

Section 2 below outlines the different procedures currently available for the analysis of ionograms, the relation between them, and development of the least-squares polynomial approach. POLAN is not always the best choice. When a simplified representation of the ionosphere is adequate, or when data can be used at a fixed series of frequencies, a simpler procedure may be more efficient as discussed in Section 3. A mathematical outline of POLAN is given in Section 4, and a general discussion of the procedures involved is in Section 5. Sections 6 to 9 discuss the start and valley

procedures employed with ordinary and with ordinary-plus-extraordinary ray data. In these regions a single defined solution is generally not possible, so physically desirable features are combined with the data in a least-squares solution. Sections 4 to 9, and Appendices A to C, summarise much unpublished work which provides the basis for the techniques used in POLAN. The practical use of POLAN is described in Section 10, while Section 11 describes a typical system for scaling, correction and analysis of ionosonde data.

Documentation of POLAN and the associated subprograms is given in Appendices D to F; these provide logic flow tables, variable descriptions and computer listings. Appendix G gives standard test data and the resulting output, so that correct operation of the main features of POLAN can be verified. The data also illustrate some of the refinements available in POLAN for obtaining maximum information and accuracy in different situations. All programs and test data are available from World Data Center A.

For a given set of virtual-height data, real-height analysis using POLAN takes roughly twice as long as a simple lamination analysis. For a given overall accuracy, however, POLAN requires only about half as many data points. Thus there is little final difference in computing time, and there can be a worthwhile saving in the time required for scaling the ionograms. No problems have been found in running POLAN on a minicomputer. About 40kB of memory are required with a PDP-11. The 24-bit accuracy of such machines is sufficient for all modes of analysis, because of the stable procedure used to solve the simultaneous equations. Comparison of results from a PDP-11 and from a larger computer with 40-bit accuracy shows very few instances in which the calculated real heights differ by more than 0.001 km.

In normal operation results are obtained using a polynomial representation of the real-height profile, fitted to several points each side of the section being calculated. This provides an accurate interpolation between scaled frequencies, which is necessary for an accurate analysis. Virtual height data define primarily the real-height gradients at the scaled frequencies. Real heights are therefore defined most accurately between the scaled frequencies (Titheridge, 1979). Thus when an accurate analysis is used to obtain real heights at the scaled frequencies, it is dealing directly with the most difficult points. Tests have shown that direct second difference interpolation is then sufficient to reproduce the profile between scaled frequencies with little or no increase in the mean error. Results obtained by POLAN are therefore normally stored as arrays giving the scaled frequencies and corresponding real heights. Some extrapolated points are added above the layer peaks, for simpler calculation of mean profiles and to give smooth plots with second or third order parametric interpolation (which is necessary to cope with non-monotonic profiles). The frontispiece shows some examples obtained with fully automatic processing and plotting of digital ionosonde data.

For some purposes a mathematical representation of the calculated profiles is convenient. This has recently been provided for in POLAN, as outlined in section 2.4 and appendix G.3. The basic architecture of POLAN is flexible and expandable. Further development depends on increased experience in defining physical constraints, on formulating judgement criteria for difficult conditions and specifying appropriate courses of action. Users of POLAN can help in this development by informing the author of difficult data types, how these might be identified, and ways in which they might best be treated. Users are also urged to register with the author so that they will receive any further information on new developments or suggested program changes.

## 2. IONOGRAM ANALYSIS PROCEDURES

### 2.1 Lamination Methods

(a) First order.

The virtual height ( $h'$ ) and the real height ( $h_r$ ), for a radio wave incident vertically on the ionosphere, are connected by the relation

$$h'(f) = \int \mu' dh. \quad (1)$$

The group refractive index  $\mu'$  is a complicated function of the wave frequency  $f$ , the plasma frequency  $F_N$ , the magnetic gyrofrequency  $F_B$  and the magnetic dip angle  $I$ . There is therefore no analytic solution of (1). For accurate calculations the integral must be determined numerically using some model for the variation of plasma frequency  $F_N$  with height  $h$ . Once this is done the virtual heights  $h_i'$ , at any required series of frequencies  $f_i$ , can be expressed in terms of the model parameters. If the virtual heights  $h_i'$  are measured, the set of equations can be inverted to obtain the parameters defining the variation of  $F_N$  with height.

The normal procedure is to use the virtual heights  $h_i'$  measured at a series of frequencies  $f_i$  (where  $i = 1$  to  $n$ ) to determine the real heights of reflection  $h_i$  at those frequencies. In the "linear lamination" method the plasma frequency  $F_N$  (or the electron density, proportional to  $F_N^2$ ) is assumed to increase linearly with height between successive observed frequencies. The model ionosphere is then defined by  $n$  parameters which are determined from the  $n$  measured virtual heights by inverting the matrix of equations relating  $h_i'$  and  $h_i$  (Budden 1955), or by using a step-by-step solution (Thomas 1959). The resulting profile is of limited accuracy, unless  $n$  is very large, with gradient discontinuities at the measured frequencies. In regions where the gradient  $dh/dF_N$  is increasing with height (as near the peak of a layer) the calculated profile is too high. The corresponding virtual-height curve agrees with observations at the measured frequencies, but is too high elsewhere.

(b) Second order.

The simplest method for improving the profile accuracy is to calculate real heights  $h_i$  at frequencies between the virtual-height frequencies. Since linear laminations define the gradient, and hence the virtual height, most accurately near the centre of the laminations, this "linear offset" analysis gives an order of magnitude improvement in the relation between real and virtual heights (Titheridge, 1979). The resulting accuracy is equivalent to that obtained by other second order techniques, while the stability of the analysis is appreciably better. Calculated points correspond to a second order analysis so that intermediate heights must be determined by second order interpolation rather than by use of the linear laminations.

The commonest second order procedure at present represents the real-height profile by a series of parabolic laminations. Successive laminations are matched at the end points, corresponding to the observed frequencies, so that both the real height and the gradient are continuous (Paul 1960, 1967; Paul and Wright 1963; Doupnik and Schmerling, 1965). The profile is then defined, as before, by  $n$  parameters which can be determined from the  $n$  measured virtual heights. Like the linear offset method, this analysis gives results which are about 10 times more accurate than those obtained from the linear lamination analysis. The results are least accurate in regions where the gradient is not varying linearly with height, as near the peak of the layers and at any points of inflection (corresponding to cusps on the virtual-height records).

### 2.2 Single-Polynomial Methods

It is not practicable to reduce errors further by using higher order expressions for the profile between calculated points, if these expressions define independent laminations which are matched only at the ends. Such a procedure becomes increasingly unstable as the order of the expressions increases; even the parabolic lamination analysis is appreciably less stable than the linear offset method. The problem is essentially one of interpolating between specified points ( $h_i, f_i$ ) to determine the integral in (1). Such interpolation is most accurately done by using expressions fitted over a number of points on either side of the interval being considered; this gives considerably greater stability than using independent high-order expressions for each interval, fitted only by matching derivatives at the end points.



The ultimate model for single-layer calculations would seem to be one which maintained the continuity of all derivatives at all points. This implies the use of a single mathematical expression to represent the entire profile. The mathematics implicit in this idea are tractable provided that the adopted expression is differentiable. For any set of scaling frequencies a matrix of coefficients can then be obtained giving the real height at each frequency directly in terms of the observed virtual heights. With the entire real-height profile represented by a single analytic expression, coefficients can be determined which give any required parameters of the real-height profile directly. Thus the peak height, the scale height at the peak and the sub-peak electron content can be obtained directly from the measured virtual heights without the need for calculating any other aspects of the profile.

Increased accuracy is obtained by requiring a parabolic peak at the observed critical frequency. For a single-layer ionogram the results are then quite acceptable with only a small number of data points; a 5-point analysis gives values of peak height which are an order of magnitude more accurate than those obtained using Kelso-Schmerling coefficients (Titheridge, 1966). Tables are available for the analysis of ionograms taken anywhere in the world, using 5 or 6 measured virtual heights (Titheridge, 1969; Piggott and Rawer, 1972). With this number of points the results are completely stable, and by choosing either the 5- or 6-point frequency grid large cusps on the ionogram can be avoided. Coefficients are also given for the analysis of night-time ionograms, using 5 ordinary and 1 extraordinary ray measurement; the resulting profile is then approximately corrected for the effects of group retardation in the night-time E region.

### 2.3 Overlapping Polynomials

Accurate calculations require accurate interpolation between observed frequencies. The Kelso method applies Gaussian interpolation to the virtual heights. In other methods interpolation is done in the real-height domain, since the real-height curve is considerably smoother. As in most problems of fitting discrete data points, accuracy is initially improved by an increase in the order of the interpolating polynomial. A limit is reached, however, beyond which the results become unstable. There is therefore an optimum number of terms ( $n$ ) for the polynomial. When the number of data points to be fitted is greater than  $n$ , a different interpolating polynomial is used for each interval. For maximum accuracy, the polynomial should be fitted to data on BOTH sides of the interval considered.

In many problems interpolation polynomials with 4 to 6 terms are about optimum. For ionogram analysis, oscillatory tendencies begin with 7 terms at large magnetic dip angles, and with 6 terms near the equator (Titheridge, 1975a). Five terms were therefore adopted for the polynomial used to represent the real-height curve between successive data points. This gives the fourth-order overlapping polynomial analysis LAPOL (Titheridge, 1967b, 1974a). In this method the real height between two given frequencies is represented by a fourth order polynomial, which is fitted to two points on either side of the interval considered. Gradients are also matched at the ends of each interval. This gives five constraints which are used to determine the five parameters for each polynomial.

Procedures can be constructed in which the polynomial is defined by real heights at a number of points on either side of the interval considered, and by specified derivatives at some of these points. Virtual heights  $h_p'$  are then expressed in terms of the polynomial coefficients, using (1), and the resulting equations inverted to obtain the real-height parameters. The computational complexity of this process can, however, become prohibitive. With fourth-order polynomials, and virtual heights measured at 60 frequencies, the 300 parameters defining the real-height profile would be obtained by solving a set of 300 simultaneous equations. This cannot be done efficiently or accurately. Matching of derivatives at frequencies above the central interval of each polynomial is therefore replaced by matching of virtual heights. There seems little if any disadvantage in this approach, which enables a simple step-by-step analysis. The virtual-height data contains all that is known about the profile; virtual-height matching therefore implies a simultaneous matching of all available information, whether this relates to true heights or to derivatives.

Successive polynomials fit the same real height at the joining points, since the real height calculated from one section is used as a constraint in the next. If two adjacent polynomials are also required to give the same virtual height at the joining point, the gradients must match closely at that point (since the virtual height at any frequency depends most closely on the gradient at that frequency). With 5-term polynomials we get 5 simultaneous equations at each step. Shifting the origin to the last calculated real height gives well-conditioned  $4 \times 4$  matrices, and errors in the matrix inversion of less than 1 part in  $10^6$  using standard 24 bit precision (Titheridge, 1967b).

In tests using a number of different real-height profiles with various frequency intervals and dip angles, the 5-term overlapping-polynomial analysis gives results which are 100 to 1000 times more accurate than using parabolic laminations (Titheridge, 1975a, 1978). The stability of the analysis,

measured by the amplitude of spurious real-height oscillations following a cusp or discontinuity in the virtual-height curve, is 20% to 50% better than for the parabolic analysis (Titheridge, 1982).

The ability to interpolate a point of inflection between successive frequencies makes the careful selection of reading frequencies unnecessary, and a fixed grid can be used for scaling ionograms. This considerably speeds up the scaling and, since coefficients need be calculated only once (for a given station) calculation of the real-height curve takes typically less than one second. Both fixed and variable frequency modes, with an optional one-point extraordinary-ray starting correction and insertion of a model E-F valley, are provided in the programme LAPOL (Titheridge, 1974a).

## 2.4 Least-Squares Solutions

Further improvement in real-height calculations requires the incorporation of more data points, which are smoothed to remove the jitter caused by random errors. This smoothing can be done manually, or by some algorithm which is applied prior to the  $N(h)$  analysis. A preferable procedure, however, is to obtain the real-height profile as a direct least-squares fit to all of the data points. In a polynomial analysis this means that the number of terms in the polynomial ( $n$ ) is less than the number of fitted data points ( $m$ ). There is no limit on the value of  $m$ , while the detail required in the profile is set independently by the value of  $n$ . As a result of the least-squares procedure, fitted polynomials are completely stable for values of  $n$  up to at least 20 (when a stable mathematical procedure is used to solve the equations).

For single-layer ionograms, all available data can be fitted in a single step. This is particularly valuable for the analysis of topside ionograms where full use can be made of fragmentary ordinary and extraordinary ray traces. These are incorporated into a single analysis which interpolates smoothly across any unobserved regions, and can give any desired number of points on the real-height profile (Titheridge and Lobb, 1977).

With daytime bottomside ionograms, single-polynomial solutions are obtained first for the E region and then for the F region. By incorporating a model valley into the analytic expression for the upper section, and using all available ordinary and extraordinary ray data for the F region, the best-fitting valley width and F region real-height profile are obtained directly (Lobb and Titheridge, 1977a). Generalisation of this approach to allow overlapping polynomials, fitting an arbitrary number of data points, yields the program POLAN described in Section 4.

In its normal form POLAN produces results giving the real heights  $h$  at the plasma frequencies  $f_N$  corresponding to the scaled data frequencies. Some studies require values for the vertical gradient of plasma density in the ionosphere. Virtual-height data define this gradient accurately at the plasma frequencies  $f_N$  corresponding to the scaled data frequencies. Real heights at these frequencies are calculated in section C5 of POLAN by the statement

$$HT(KRM) = HA + SUMVAL (MQ, Q, DELTF, 1)$$

where  $DELTF = f_N - FA$ . Preceding this statement with a line

$$GRAD(KRM) = SUMVAL (MQ, Q, DELTF, 2)$$

will store correct values for the gradients  $dh/df_N$  at the same frequencies. The array GRAD must be added to the POLAN parameters, with the same dimension as the present frequency, height arrays FV and HT.

A recent modification to POLAN can provide a consistent mathematical representation for each calculated profile. Real-height polynomials of any required order (up to 15 for the final layer, or 10 for lower layers) are obtained for each layer, as outlined in appendix G.3. Results are exactly the same as if Chebyshev polynomials (of the same order) had been used, since both provide the unique solution with the best least-squares fit to the virtual-height data. A separate polynomial is required for the E layer, and also for the F1 layer if it has a distinct critical frequency, since polynomials in  $f_N$  cannot include a valley. 5 or 6 terms are generally adequate for the E or F1 layers, with about 8 terms for the F2 layer. The constant term in each expression is suitably adjusted to allow for any valley, as described in section G.3.

### 3. SELECTION OF AN $N(h)$ METHOD

Choice of an appropriate method of  $N(h)$  analysis depends on the amount and accuracy of the desired profile information. This in turn is dictated by the application. Three main groups, requiring different levels of accuracy, may be distinguished and are discussed in 3.1 to 3.3 below. A fourth area is the automated analysis of digital ionograms. This requires additional program checks for poor or nonsensical data, to prevent premature program termination, and methods for dealing correctly with Sporadic E reflections. A modified subroutine DPOLAN has been developed for this purpose and is available (with little documentation) from the author.

#### 3.1 Rapid Estimation of Layer Constants

Some studies require only first-order estimates of the height and thickness of the ionospheric layers. These would include the examination of large-scale variations, or the correction of other measurements (such as total electron content and transionospheric U.H.F. propagation) for the approximate effects of the sub-peak ionosphere. The rapid single-polynomial analysis was designed specifically for such purposes. Only 5 or 6 virtual heights need be scaled, at frequencies defined by a grid onto which the ionogram is projected. The measurements may be processed on a programmable calculator using published coefficients (Titheridge, 1969), or with a simple computer program and coefficients calculated (or obtained from the author) for a particular site. Results give directly the peak height of the layer, the scale height at the peak, the sub-peak electron content, and the approximate real heights at the scaled frequencies.

The method and the scaling frequencies are designed for maximum accuracy, with minimum effort, near the peak of a layer. In this region results approach those from a normal monotonic lamination analysis. Real heights are not accurate near the peak of an underlying layer, particularly when there is an appreciable valley between the two layers. This is an inevitable result of the smoothed representation used at lower frequencies. Thus when realistic profile shapes are required across underlying peaks or cusp regions the single-polynomial analysis should not be used.

The accuracy of the single-polynomial analysis has been investigated by McNamara (1976), by comparing the results with true profiles including (for the daytime F layer) an underlying E-F valley. Results should more appropriately be compared with the equivalent monotonic profile, since this is what the method is attempting to emulate. The larger errors obtained near the valley region are then removed. Correctly used the single-polynomial analysis gives good estimates of the main characteristics of the ionospheric layers, and saves a great deal of time when more detailed profile information is not required.

#### 3.2 Calculation of Monotonic Profiles

Many studies require some knowledge of the variation of electron density with height below the peaks of the layers, but are satisfied with a monotonic representation. This category has, perforce, included most studies to date, since few current procedures will consistently allow for low-density or valley ionisation. Neglect of the low-density (underlying) ionisation is most serious at night, when only the F layer is observed. Results are then typically 5 to 50 km too high at the lowest frequencies, and 1 to 10 km too high at the layer peak. Neglect of the valley between the daytime E and F layers gives calculated heights which are commonly 10 to 50 km too low at frequencies above foE, and about 5 km too low near the peak of the F layer. The errors due to these unobserved regions vary smoothly with frequency; at frequencies more than 1 MHz above  $f_{min}$  (night) or foE (day) the real-height errors vary approximately as  $1/f^2$ .

Reasonably accurate monotonic profiles require virtual-height data at frequency intervals of about 0.1 to 0.5 MHz. The smaller intervals are used near foE, and possibly near foF1 and foF2. The total number of points scaled is commonly between 15 (at night) and 50 (for day-time ionograms with several cusps) when a polynomial analysis is used. The linear lamination method needs considerably smaller frequency intervals to avoid systematic errors in regions of large profile curvature. Several alternative procedures are available which reduce this curvature error by a factor of 20 to 100, with little increase in computing time or complexity. A good example is the parabolic lamination analysis described by Paul (1977). The linear offset procedure (Titheridge, 1979) gives similar results with a very compact program.

Use of the overlapping-polynomial program LAPOL (Section 2.3) can reduce costs appreciably. The ability to change profile curvature between scaled frequencies gives greater accuracy, and makes the choice of scaling frequencies less important. Virtual heights may therefore be scaled at fixed frequencies, and analysed with precalculated coefficients (Titheridge, 1967b, 1974a). This gives an extremely fast analysis (one second per ionogram, on a minicomputer) at the cost of a somewhat larger

program than the preceding methods. Provision is made for a starting correction, using a single extraordinary ray point or the mean models of Section 6, and for inclusion of a model valley. LAPOL therefore provides a useful alternative to POLAN where speed, simple (manual) scaling and cost are important. Digital ionosondes providing large amounts of data at a fixed series of closely-spaced frequencies can also be analysed rapidly using the pre-calculated coefficients of LAPOL, in cases when the full incorporation of extraordinary ray data is not feasible or necessary.

When reduction of fluctuating errors is of prime importance an overlapping-cubic analysis (Titheridge, 1982) should be used. This is completely free from the spurious oscillations which can occur with parabolic or, to a lesser extent, with polynomial methods, as discussed in Appendix A.2. The overall accuracy is appreciably less than that obtained with the higher order modes in POLAN, but is somewhat better than with parabolic laminations. The cubic analysis can be programmed directly, or is available (with full start and valley treatments) as Mode 3 of POLAN.

### 3.3 Full Calculations

For many studies the calculated electron-density profile must be as accurate and reliable as possible, given the vagaries of ionosonde data. A least-squares analysis is required, with adjustable range for the overlapping real-height sections, adjustable weights for the data points, and a least-squares calculation of all layer peak parameters. The largest errors are then due to the unobserved regions, at frequencies below  $f_{min}$  and in the valley between two layers.

Use of a starting correction to allow for low-density underlying ionisation is particularly important at night. The problem cannot be avoided by obtaining virtual-height data from the night-time E layer, since the E and F layers are generally separated by a wide valley. Extrapolation of the ordinary ray trace is also unreliable: increased underlying ionisation will often increase an extrapolated starting height, when it should be decreased. A true starting correction requires extraordinary-ray measurements at frequencies well below the critical frequency of the lowest observed layer, so that retardation relates primarily to the underlying ionisation. If suitable data are not available some mean model for the underlying ionisation must be used. This has been discussed recently by McNamara (1978a, 1979), and corrected models are given in Sections 6.3 and 6.4 of this report.

Allowance must be made for the presence of a valley between the daytime E and F layers. Using combined ordinary and extraordinary ray data, profile heights can be calculated which are correct to within a few km at the base of the F layer, and to within 1 km near the peak. In most cases only one meaningful valley parameter can be determined; this corresponds most closely to the overall width, or the total electron content (Lobb and Titheridge, 1977a). The analysis procedure should therefore assume some fixed, reasonably realistic model for the shape of the electron-density variation in the valley region. Combined ordinary and extraordinary ray data are then used to determine, primarily, the overall width of the valley. Useful calculations require (i) that the value of  $f_oE$  is known to within about 1%; (ii) that F-layer traces are available for both rays at frequencies sufficiently close to  $f_oE$  that the E layer group retardation is apparent; and (iii) that there are no large horizontal variations in the ionosphere. When the necessary data are not available, the analysis should include some standard valley correction. Physical criteria can be included in the solution to give an improved estimate of the most likely correction, as discussed in Section 7.3.

POLAN was designed to fulfil the above requirements, and does so to a greater extent than other current procedures. Results are obtained by a one-pass analysis under all conditions, and physical criteria are introduced to control variations in the observed regions. It therefore seems the preferred method for accurate studies.

## 4. A GENERALISED FORMULATION

### 4.1 Outline

All methods of analysis mentioned above can be considered as polynomial techniques, differing only in the order of the polynomial and in the applied constraints. Thus the linear lamination approach determines a first-order polynomial fitted to the last calculated real height and the next virtual height. The parabolic lamination analysis uses a second-order polynomial fitting the real height and gradient at the last calculated point, and the virtual height at the next. The fourth-order overlapping polynomial analysis fits the two previous real heights, the virtual height at the last calculated point, and the virtual heights at the next two points.

To encompass these and any further desirable extensions to higher orders, analysis procedures have been formulated in a completely general form. This is described in Section 4.2, where the equations are given which define a polynomial of order  $NT$ , fitting  $NR$  real heights and  $NV$  virtual heights. By specifying different values for  $NT$ ,  $NR$  and  $NV$  we obtain polynomial methods of any desired order, including the linear and parabolic lamination methods. If  $NR = 0$ , and  $NV$  is the total number of virtual-height observations, we have a single polynomial analysis. In all cases use of  $NT = NR + NV$  gives profiles which exactly fit the virtual-height data.

Setting  $NT$  less than  $NR + NV$  gives a least-squares solution. This opens up a range of possible methods which incorporate some smoothing of the experimental data. Use of a least-squares procedure removes the difficulty which occurs when a large number of virtual heights is used, that if the frequency interval is made too small then errors in the virtual heights give an unrealistic jitter in the calculated real heights (e.g. Becker, 1967). Least-squares modes should thus be particularly valuable for use with digital ionosondes. The ability to obtain a least-squares result over any section of the profile can also be exploited to good effect in coping with the start and valley problems.

When a large number of data points is available, there is no need to use a separate polynomial for each interval between scaled frequencies. Expressions fitted over any desired frequency range can be used to calculate a further  $NH$  real heights. Current lamination procedures use  $NH = 1$ . With digital ionosondes or automatic scaling procedures, larger values may be employed with advantage. Thus if the amount of available data is increased by a factor of 3, polynomials may be fitted over the same frequency range as before (which will now involve 3 times as many data points) with each successive step in the analysis calculating 3 new real heights.

Observed virtual heights are affected by the amount of underlying ionisation, with plasma frequencies less than the lowest observed frequency  $f_{min}$ , and by the size of any valleys between the ionospheric layers. To within normal experimental accuracy the effect of these regions can be defined by two suitably chosen parameters (Section 8). So for starting or valley calculations, two additional terms are added to the real-height expression; these represent basically the total amount of "unseen" ionisation, and the ionisation gradient near the top of the unobserved region. When only ordinary ray data are available, these terms are obtained from some mean model of the underlying or valley region. With suitable extraordinary ray measurements, at  $NX$  frequencies say, we get  $NV + NX$  equations from which to determine  $NT + 2$  real-height coefficients (where  $NT$  is the number of terms in the polynomial real-height expression). For reliable results the ordinary and extraordinary ray data should correspond to similar plasma frequencies at reflection, and a least-squares analysis is used with  $NT + 2 < NV + NX$ .

### 4.2 The Basic Equations

At each step in the analysis, the variation of plasma frequency  $FN$  with height  $H$  is given by:

$$H - HA = \sum_{j=1}^{NT} q_j \cdot (FN - FA)^j \quad (2)$$

The point  $FA, HA$  is the origin for the real-height polynomial. It is assumed that the real-height profile is known up to the height  $HA$ ; and that the virtual heights at frequencies greater than  $FA$  have been corrected for the group delay of the rays in the underlying sections, to give the reduced virtual heights  $h''$ . The value of  $NT$  (the number of terms in the polynomial real-height expression) defines the order of the analysis.

If we have progressed  $k$  points through the real-height profile, then  $FA = f_k$  and  $HA = h_k$ . Equation (2) is used to calculate the real and virtual heights at the frequencies  $f(k+i)$  for  $i = 1$  to  $NV$ , where  $NV$  is the number of virtual heights fitted in each step. Writing  $F_i = f(k+i)$  we have

$$\begin{aligned} h''(k+i) - HA &= \int \mu'(F_i, FN).dh/dFN.dFN \\ &= \sum_{j=1}^{NT} q_j . B(i, j) \end{aligned} \quad (3)$$

where

$$B(i, j) = \int_{FA}^{FR} \mu'(F_i, FN). (FN - FA)^{j-1} dFN. \quad (4)$$

$FR$  is the plasma frequency at reflection, equal to  $F_i$  for the ordinary ray or to  $(F_i(F_i - FB))^{0.5}$  for the extraordinary ray.

Real height coefficients  $C(i, j)$  are also calculated such that

$$h(k+i) - HA = \sum_{j=1}^{NT} q_j . C(i, j) \quad (5)$$

where

$$C(i, j) = (F_i - FA)^j. \quad (6)$$

These coefficients are determined for frequencies  $F_i$  from  $f(k+1)$  to  $f(k+NV)$ . Setting  $B(i+NV, j) = C(i, j)$  we have the set of equations

$$\begin{aligned} B(1,1)q_1 + B(1,2)q_2 + \dots + B(1,NV)q_{NT} &= h''(k+1) - HA \\ B(2,1)q_1 + B(2,2)q_2 + \dots &= h''(k+2) - HA \\ \vdots & \\ B(NV,1)q_1 + B(NV,2)q_2 + \dots &= h''(k+NV) - HA \\ B(NV+1,1)q_1 + B(NV+1,2)q_2 + \dots &= h(k+1) - HA \\ \vdots & \\ B(2NV, 1)q_1 + B(2NV, 2)q_2 + \dots &= h(k+NV) - HA \end{aligned} \quad (7)$$

These may be written

$$[B].[Q] = \begin{bmatrix} H'' \\ H \end{bmatrix} \quad (8)$$

where  $[B]$  is a  $2NV \times NT$  matrix,  $[Q]$  is a  $NT \times 1$  column vector, and  $H''$ ,  $H$  are  $NV \times 1$  column vectors. Numerical calculation of the coefficients  $B(i, j)$  using the subroutine COEFIC is described in Appendix D.1.

In the real-height vector, only the first  $NR$  values are known (where  $NR$  depends on the mode of analysis). Thus right-hand sides are known for the first  $NV+NR$  rows in (8), corresponding to the first  $NV+NR$  equations in the set (7). These rows are solved to obtain the parameters  $q_j$  which define the real-height polynomial (2). Using these parameters the next  $NH$  rows are evaluated to give  $NH$  real heights;  $NH$  is generally equal to 1 but can be greater for the first polynomial (Section 6) and for higher order modes (Section 5.3). The index  $k$  is incremented by the number of new real heights calculated, giving new values for  $FA$  and  $HA$ , and the process repeated until the entire real-height curve has been calculated.

A linear lamination analysis is obtained by setting  $NT = NV = 1$  and  $NR = 0$ . Thus at each step a first order polynomial is determined, extending from the last known real height and fitted to the next virtual height. The parabolic lamination procedure is obtained by setting  $NT = 2$ ,  $NV = 1$  and  $NR = -1$ . The  $-1$  is used as an indicator in the program to use a gradient expression

$$\sum_j (FN - FA)^{j-1} . q_j = GA$$

after the single virtual-height equation and before the single real-height equation in the set (7).  $GA$  is the gradient at  $FA$  calculated from the previous polynomial. This departure from the normal scheme is to give exact agreement with the standard parabolic-lamination analysis, which matches gradients rather than virtual heights at the end points.

Higher order methods of analysis are obtained simply by increasing the values of  $NT$ ,  $NV$  and  $NR$ . For the standard fourth-order overlapping polynomial analysis (Titheridge, 1967b) we set  $NT = 4$ ,  $NV = 3$  and  $NR = 1$ . This gives a five term polynomial (including the constant), fitted to the last two calculated real heights  $h(k)$  [ $= HA$ ] and  $h(k+1)$ , and to the three virtual heights  $h'(k+1)$ ,  $h'(k+2)$ , and  $h'(k+3)$ . The real-height expression for  $h(k+3)$ , available in the set (7), is not specifically required. It does, however, give a good estimate of this height so that the correct value of gyrofrequency can be used for the next step in the analysis.

### 4.3 Calculation Procedures

The subroutine COEFIC (Appendix D.1) is called at each step to calculate the coefficients  $B(i,j)$  for the simultaneous equations (7). For the real-height conditions (5) the coefficients are simple functions of frequency. The virtual-height equations involve group index integrals (4), which are evaluated using 5- or 12-point Gaussian integration depending on the desired accuracy. At high latitudes both 5 and 12 point integrals are employed, over different sections of the integration range, in a way which reduces errors by a factor of 10 to 100 at dip angles of  $78$  to  $88^\circ$  (Appendix B.3). At a given frequency the  $NT$  polynomial integrals are obtained from the same 5, 12 or 17 calculated values of  $\mu'$ . Calculation time therefore depends primarily on the number of virtual heights ( $NV$ ) fitted at each step, and not on the number of terms in the fitted polynomial.

Solution of the simultaneous equations is carried out by the subroutine SOLVE (Appendix F.4). This gives an exact solution if  $NT = NV+NR$ , and a least-squares solution if  $NT < NV+NR$ . The calculation uses orthogonal Householder transformations, giving accurate results for values of  $NT$  up to at least 15. From the calculated real-height coefficients any required features of the profile (such as the heights or gradients at any required frequencies, and the total electron content) can be obtained.

For least-squares solutions we want the calculated polynomial to agree closely with the  $NR$  known real heights, and less accurately with the given virtual heights. This is accomplished by multiplying the first  $NV$  rows in (7) by a weighting factor  $WVIRT$ . Tests show that  $WVIRT$  should be less than 0.1 for good matching of successive polynomials under all conditions. The value  $WVIRT = 0.05$  has therefore been adopted. The relative fitting accuracies of the virtual and real heights depends on the square of this weight, and also on the square of the relative size of the coefficients  $B(i,j)$  in the equations (7). Combining these effects gives a relative fitting accuracy of about 0.02. Thus for a typical analysis using real (inaccurate) data a calculated least-squares polynomial will fit the previously determined real heights to within about 0.01 km, and will agree with the virtual-height data to within 0.5 km.

When an exact polynomial fit is being used ( $NT = NV+NR$ ) or when real-height equations are not included in the set being solved (as in the start or valley calculations) the value of  $WVIRT$  has no effect on the results. When extraordinary ray data are being used to overcome the starting or valley ambiguity additional weights are used to give slightly less importance to the extraordinary ray measurements, and greater importance to the last ordinary ray virtual height to ensure a smooth continuation with following ordinary ray measurements.

## 5. THE PROGRAM POLAN

### 5.1 General Characteristics

The Fortran program POLAN has been constructed using a small number of generalised subroutines. This allows many different modes of analysis, and changes in mode can be made at any time. Calculations normally proceed in a stepwise fashion to obtain successive, overlapping sections of the real-height profile. At any given stage calculations are referred to a known real-height point FA, HA called the origin. The next real-height section passes through the origin, and is defined by the polynomial expression

$$h - HA = \sum_{j=1}^{NT} q_j (FN - FA)^j \quad (9)$$

Different modes of analysis are then specified in terms of the following parameters:

- NT = the number of coefficients  $q_j$  in the polynomial real-height expression;
- NV = the number of virtual heights used in each step;
- NR = the number of known real heights used in each step;
- NH = the number of new real heights to calculate from the polynomial expression.

Calculations begin from some defined starting point  $(f_s, h_s)$ , where  $f_s$  is normally less than the lowest scaled frequency  $f_1$ . For the first step of the analysis (the calculation of the first polynomial segment) no further real heights are known, so that  $NR = 0$ . The analysis can use any number of virtual heights (NV) to calculate any required number of real heights (NH,  $\leq NV$ ). Thus the fourth-order analysis obtains three real heights ( $h_1$  to  $h_3$ ) by fitting a four-term polynomial from the point  $(f_s, h_s)$  to the first four virtual heights. For the next step the origin is advanced two points, to  $(f_2, h_2)$ . One further real height is then known and successive polynomials are determined using  $NT = 4$ ,  $NV = 3$  and  $NR = 1$ .

When the origin for the real-height expansion is at the  $k^{\text{th}}$  point in the array of frequencies (FV) and heights (HR), we have  $FA = FV(k)$  and  $HA = HR(k)$ . The coefficients in the real height expansion are then determined by the real heights  $HR(k+1)$  to  $HR(k+NR)$ , and the virtual heights  $HV(k+1)$  to  $HV(k+NV)$ . This provides  $NR+NV$  constraints to determine the NT coefficients  $q$ . If  $NT = NR+NV$  we have an exact solution, and if  $NT < NR+NV$  we get a least-squares solution. The number of terms NT which can be used for a real-height expansion is limited to 15 in POLAN, by the dimensions of the arrays B and Q. The total number of constraints ( $NR+NV$ ) is similarly limited to 30.

The real-height expansion is not continued across a critical frequency in any mode. A critical frequency or cusp is indicated by a virtual height of less than 30 (as described in Section 5.4). When this is encountered the value of NV is reduced to equal the number of available virtual height measurements before the critical frequency. For Mode 10 (a single-polynomial analysis) NV is normally reduced from the maximum specified value (30) to the number of data points available before the next critical frequency. Thus with a multi-layer ionogram, each layer is represented by a separate analytical expression.

An important question in real-height calculations is the presence of instabilities in the results, as shown by the presence of spurious oscillations. Only Mode 1 (linear laminations) and Mode 3 (overlapping cubics) are completely free from this effect. All modes which maintain some continuity of gradient between successive sections give some spurious oscillations when used to analyse irregular virtual-height data. This question has been investigated by considering the form of real height curves fitted to discontinuous data; by analysing virtual-height data corresponding to idealized delta, step and ramp type discontinuities; and by the analysis of typical cusped ionograms (Titheridge, 1982). In all cases the amplitude of spurious oscillations is largest for Mode 2 (the parabolic lamination analysis) in which successive segments are matched only at the end points. Compared with Mode 2, oscillations are 20% to 60% less for Mode 4, and 50% to 90% less for the higher order least-squares modes.



## 5.2 The Standard Modes of Analysis

Ten standard modes of analysis are provided in POLAN. These use values of NT, NV, NR and NH defined in the data arrays IT, IV, IR and IH. Other modes can be used, if desired, by simply changing the constants in these arrays. Each array contains 20 values. The first ten are used for the first real-height expansion, at the beginning of the analysis or after a peak, when no further real heights are known and NR = 0. At the end of this first step, after NH real heights have been calculated and the index k advanced by this amount, k is stepped back by a number given in the data array IR. Thereafter the second ten values in the arrays IT, IV, IR and IH define the values of NT, NV, NR and NH to be used in continuing the analysis. The values of these constants for each mode are listed in Table 1, with a brief outline of the resulting analysis.

Real-height sections determined by the different standard modes of analysis are illustrated in Fig. 1. Vertical lines show the origin of the expansion at the frequency FA. Solid dots represent known real heights, open circles are calculated real heights, and crosses represent fitted virtual heights. Mode 1 corresponds to the linear lamination analysis, in which a linear section is calculated from the last known real height to fit the next virtual height. Thus we calculate a polynomial with NT = 1 terms, using NR = 0 further real heights and NV = 1 further virtual heights; the result is used to determine NH = 1 further real heights. The new section of the real-height profile which is determined in this step is shown as a heavy line in Fig. 1.

A negative value of NR is used in some modes. This signals that one of the real heights to be fitted is at the frequency just below FA. This is the case for Mode 3 and Modes 5 to 9 in Fig. 1. An exception is made of Mode 2; to give exact agreement with the normal parabolic lamination analysis, NR = -1 here is taken to mean that the gradient dh/dFN is fitted at the frequency FA. Mode 2 then calculates a polynomial with NT = 2 terms fitting the initial gradient (as determined from the previous lamination) and the next virtual height.

Mode 4 corresponds to the five-term overlapping polynomial analysis described previously (Titheridge, 1967b). In the present context this reduces to NT = 4 terms to be determined in the expansion (2), since the constant is automatically set to make the polynomial pass through the point (FA,HA). The four terms are determined from the next one real-height and three virtual heights. The polynomial is, therefore, fitted to data covering three successive frequency intervals as shown in Fig. 1. The result is used to calculate a further section of the real-height curve over the centre interval shown by a heavy line. This is somewhat similar to a representation by spline functions, with the polynomial function in each interval matching adjacent functions in both value and gradient at the end points and in value at one further point each side. In the present implementation, however, gradient matching is replaced by virtual height matching (which it closely resembles) and the additional point fitted at the high frequency end is a virtual height and not a real height. These changes make possible the stepwise solution which can cope with any number of data points.

For each of Modes 1 to 4 we have  $NT = NV + |NR|$ . Thus the number of terms determined is equal to the number of constraints, and the resulting profile will match the given virtual-height data exactly (apart from the effect of limited numerical accuracy in the calculations). For each of Modes 5 to 10,  $NT < NV + |NR|$  and we get a least-squares solution. The calculated polynomials pass exactly through the origin (the known point FA,HA), but will not in general give an exact fit to the virtual-height data. A good fit to the previously calculated real heights is imposed by giving greater weight to the real-height equations (as discussed in Section 4.3).

Mode 5 gives the procedure currently recommended for most purposes. This uses a polynomial fitted over two frequency intervals on either side of the real-height section to be determined. It gives appreciably greater accuracy than Mode 4, and slightly worse in general than Mode 6.

Modes 7 to 9 are similar to Mode 6, except that each calculated real-height segment covers two or three data points. Thus the polynomials are obtained from a least-squares fit to a larger number of points, and are used to calculate two or three real heights at each step. This gives a faster analysis with smoother results. These procedures should be suitable for analysing data from digital ionosondes, when large numbers of data points are available. With irregular data it could be desirable to reduce the number of terms in the polynomial; thus an analysis of the type shown for Mode 9, but with NT reduced to about 5, will use three times the normal amount of data and produce only the normal amount of resolution in the results.

Mode 10 determines a single analytic real-height expression for each layer. It is defined in POLAN by NT = 73, NV = 30, NR = 0 and NH = 30. This permits up to 30 virtual-height data points to be included in the analysis. The limit is set by the dimensions of the array B(32,17) in POLAN, and can be changed to enable any number NMAX of virtual heights to be used by altering the first dimension to NMAX+2. Values of NT > 20 are interpreted in POLAN as giving a percentage of (NV+2); thus Mode 10 as currently defined uses  $NT = 0.73(NV+2)$  terms in the analytic real height expression. This always gives a least-squares solution, including all the ordinary and extraordinary ray data for a given layer.

**Table 1.** The standard modes of analysis incorporated in POLAN and in SPOLAN, as illustrated in Fig. 1. The polynomials used have **NT** terms, plus the constant term which is automatically included by taking the origin for the polynomial at a known real-height point FA,HA. These terms are determined by a (least-squares) fit to the virtual-height data at the next **NV** frequencies above FA, and to known real heights at **NR** frequencies above FA. If NR is negative, the fit is to one real height below FA, and  $|NR|-1$  real heights above FA. **NH** gives the number of new real heights calculated at each step.

| MODE | NT   | NV | NR | NH | DESCRIPTION  |
|------|------|----|----|----|--|
| 1    | 1    | 1  | 0  | 1  | The normal linear lamination analysis.   |
| 2    | 2    | 1  | -1 | 1  | Parabolic laminations, fitting the last real height and gradient.  |
| 3    | 3    | 2  | -1 | 1  | Overlapping cubics, fitting no previous gradients or virtual heights and so completely free of oscillations.   |
| 4    | 4    | 3  | 1  | 1  | The five-term overlapping-polynomial analysis described in Radio Science 1967 p.1169, in which 5 terms (including the constant) fit 3 virtual plus 2 real points (including HA). |
| 5    | 5    | 4  | -2 | 1  | A six-term fit to 3 real and 4 virtual-height data points; the first least-squares analysis and the normal default procedure.  |
| 6    | 6    | 5  | -3 | 1  | A 7-term least-squares fit to 4 real and 5 virtual heights; slightly more accurate (and slower) than Mode 5 in general.  |
| 7    | 6    | 7  | -3 | 2  | 7 terms fitted to 4 real and 7 virtual height points, advancing two points at each step.   |
| 8    | 6    | 8  | -4 | 2  | 7 terms fitted to 5 real and 8 virtual heights, advancing 2 points at each step; for smoothing and analysis of dense data.   |
| 9    | 7    | 13 | -6 | 3  | 8 terms fitted to 7 real and 13 virtual heights, advancing 3 points at each step; for smoothing and analysis of high-density data.   |
| 10   | (73) | 30 | -3 | 28 | A single polynomial, with $NT = 0.73(NV+2)$ terms, fitted to all NV heights for each layer. (Current limits are $NV < 30$ , $NT < 28$ ).   |

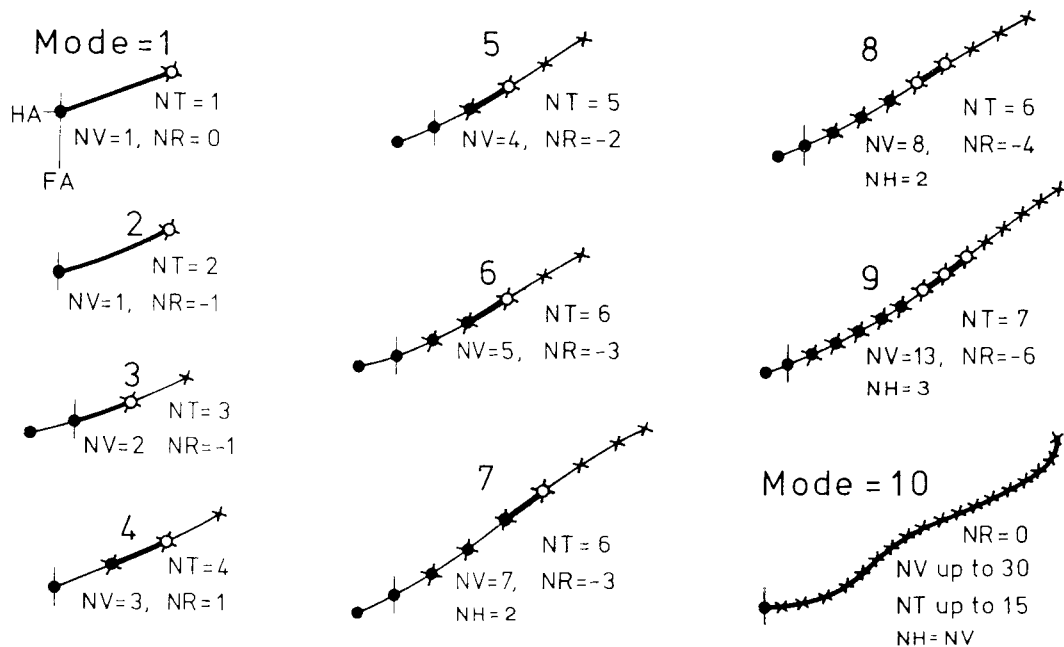


**Figure 1.** The standard modes of analysis in POLAN. Vertical lines show the origin of the polynomial real-height expression, of **NT** terms, which is calculated to fit **NV** virtual heights (shown by crosses) and **NR** known real heights (solid dots). Real heights which are calculated from the polynomial expression are shown as circles.

The time taken by an analysis depends primarily on the number of group refractive index calculations, and hence on the number of virtual-height calculations. Each cross in Fig. 1 represents a frequency at which the virtual-height integral must be evaluated, to advance the analysis one step. The time depends only slightly on the number of terms used in the real-height expansion, since (for a given  $i$ ) all the terms  $B(i,j)$  where  $j = 1$  to  $NT$  are obtained from the same set of group indices (Appendix D.1). The overall time for each mode is, therefore, roughly proportional to the value of  $NV$ , divided by the value of  $NH$  (the number of new real heights calculated at each step). This gives the approximate relative times  $NV/NH$  listed for each value of  $MODE$  in Table 2. Following columns give the measured times for the analysis of an ionogram with 20, 40, 60 or 90 scaled data points, on a Burroughs B6700 computer. The first set of times is obtained by specifying a value of  $MODE$  from 1 to 10. This gives five-point integrals (except for Modes 9 and 10) which are generally adequate at low and medium latitudes. As shown at the bottom of Table 2 the mean times for modes 1 to 8 are given (to within a few percent, at  $N > 20$ ) by the expression  $T = 60N + 0.8N^2$  msec, where  $N$  is the number of virtual-height data points.

For maximum accuracy 12-point integrals are specified, by calling POLAN with the value of  $MODE$  increased by 10 (Appendix D.1). Modes 9 and 10 always use 12-point integrals, since they include a large number of data points at each step, so times and results are the same whether Mode 9, 10 or Mode 19, 20 is specified. A zero value for  $MODE$  uses the default value  $MODE = 5$  at dip angles up to  $60^\circ$ ; this changes automatically to  $MODE = 15$  (for 12-point integrals) at dip angles of  $60^\circ$  or more. Modes 9 to 20 also shift automatically to 17-point integration when required, to maintain accuracy at dip angles up to  $90^\circ$  (Appendix B.3). Using 12-point integrals the mean times in Table 2 are approximately equal to  $T = 80N + 0.8N^2$  msec. Thus for a normal mix of 5 and 12-point integrals, changes in the number  $N$  of scaled virtual heights causes the time required for a real-height calculation to vary approximately as  $N(1+N/90)$ .

### 5.3 Curve Fitting Procedures

The accuracy of real-height calculations depends on the accuracy with which we represent the shape of the profile, between the frequencies at which virtual heights are known. All high-order modes of polynomial analysis are designed to fit one or more virtual heights beyond the point at which the next real height is to be calculated. Thus the shape of a calculated profile segment is determined using data from both sides of the segment, rather than from only the known (lower) part of the profile. This corresponds to the use of central rather than one-sided interpolation, for estimating gradient changes in the calculated section, and is the main reason for the increased accuracy and flexibility of overlapping-polynomial methods.

The different modes in POLAN correspond to different selections of the points to be fitted at each step of the calculation. A polynomial expression, with  $NT$  terms, is fitted to data at a succession of given frequencies  $F_i$ . The origin of the polynomial is taken at the frequency  $F_0$ , and the fitted frequencies correspond to values of  $i$  from 0 or -1 up to  $NV$ . Over approximately the first half of this range, fitting is to previously-calculated real heights. At all values of  $i$  from 1 to  $NV$  the polynomial is fitted to values of virtual height  $H'_i$  (corrected for group retardation due to ionisation at plasma frequencies less than  $F_0$ ). Thus in the first half (approximately) of the range the polynomial is required to have the same real height and the same slope as the previously-calculated sections. In the second half of the range only virtual-height data are known. This does, however, contain all the information which is available about the profile, so by fitting the virtual-height data we are matching all available information.

For modes 1 to 4 the number of polynomial terms which define each real-height section is equal to the number of heights (real and virtual) included in the analysis. The result is therefore an exact fit to the  $NV$  virtual heights and  $NR$  known real heights. With the higher order modes the number of defining quantities ( $NV + |NR|$ ) is greater than the number of terms  $NT$  used in the real height expansion (9). This gives a least-squares fit, with some smoothing of the virtual-height data. Real-height equations are given a larger weight in the analysis, so that the known real heights are fitted almost exactly.

Virtual-height points at each end of a calculated profile segment (the heavy lines in Fig. 1) should be fitted accurately. Points at higher and lower frequencies are required only to indicate the general trend of the profile, and are given less weight in least-squares modes of analysis. This causes the gradients at the ends of the calculated segment to be defined more closely, at the expense of points further away. Individual data points also enter and pass out of the calculation region more gradually, when the weights are varied, so that spurious fluctuations are minimised.

The effective weights given to the real and virtual-height data points are shown in Table 3, for each of the least-squares modes of analysis. For real-height points the weight is effectively infinite at  $F_0$ , corresponding to the origin  $(FA, HA)$  in (9). The weight is large at known real

**Table 2.** Calculation times in seconds, for the analysis of ordinary-ray virtual-height data with 20, 40, 60 and 90 scaled points using a Burroughs B6700 computer.

| MODE                   | NV/NH | Five-point integrals |     |      |      | 12-point (MODE+10) |     |      |      |
|------------------------|-------|----------------------|-----|------|------|--------------------|-----|------|------|
|                        |       | N = 20               | 40  | 60   | 90   | N = 20             | 40  | 60   | 90   |
| 1                      | 1     | 0.6                  | 1.5 | 3.1  | 6.2  | 0.7                | 1.8 | 3.5  | 6.8  |
| 2                      | 1     | 0.7                  | 1.7 | 3.5  | 6.6  | 0.8                | 2.0 | 3.9  | 7.3  |
| 3                      | 2     | 0.9                  | 2.4 | 4.5  | 8.4  | 1.2                | 3.0 | 5.4  | 9.7  |
| 4                      | 3     | 1.2                  | 3.2 | 5.8  | 10.3 | 1.6                | 4.0 | 7.2  | 12.3 |
| 5                      | 4     | 1.6                  | 4.2 | 7.7  | 13.3 | 2.2                | 5.4 | 9.6  | 16.0 |
| 6                      | 5     | 1.7                  | 4.8 | 8.5  | 15.2 | 2.4                | 6.2 | 10.6 | 18.0 |
| 7                      | 3.5   | 1.2                  | 3.3 | 5.8  | 10.7 | 1.6                | 4.0 | 7.0  | 12.1 |
| 8                      | 4     | 1.8                  | 4.7 | 8.5  | 15.2 | 2.5                | 5.7 | 10.0 | 17.0 |
| 9                      | 4.3   | 3.1                  | 8.1 | 14.4 | 24.5 | 3.1                | 8.1 | 14.4 | 24.5 |
| 10                     | 1     | 2.1                  | 2.8 | 4.2  | 8.4  | 2.1                | 2.8 | 4.2  | 8.4  |
| Mean for Modes 1-8     |       | 1.3                  | 3.6 | 6.5  | 11.8 | 1.8                | 4.5 | 7.9  | 13.6 |
| cf. $(60+.8N)N/1000 =$ |       | 1.5                  | 3.7 | 6.5  | 11.9 |                    |     |      |      |
| $(80+.8N)N/1000 =$     |       |                      |     |      |      | 1.9                | 4.5 | 7.7  | 13.7 |

**Table 3.** Fitted real heights H and reduced virtual heights V for the least-squares modes of analysis 5 to 10. Values of  $F_n$  refer to the nth frequency in the current step, measured from the origin at  $F_A = F_0$ . Asterisks show additional real heights to be calculated at each step, with dashes indicating the profile segment which must be interpolated accurately. The numbers under each H and V indicate the total relative effective weight given to that quantity in the calculation. Weights o are effectively infinite.

| Frequency:      | F-1 | F0  | F1  | F2  | F3  | F4  | F5  | F6  | F7  | F8  | F9   | F10 | F11 | F12 | F13 |  |  |  |  |
|-----------------|-----|-----|-----|-----|-----|-----|-----|-----|-----|-----|------|-----|-----|-----|-----|--|--|--|--|
| <b>MODE 5</b>   |     |     |     |     |     |     |     |     |     |     |      |     |     |     |     |  |  |  |  |
| Real ht:        | H-1 | H0  | H1  | --- |     |     | *   |     |     |     |      |     |     |     |     |  |  |  |  |
| Weight:         | 4   | o   | 20  |     |     |     |     |     |     |     |      |     |     |     |     |  |  |  |  |
| Virt. ht:       |     |     | V1  | V2  | V3  | V4  |     |     |     |     |      |     |     |     |     |  |  |  |  |
| weight:         |     |     | 1.0 | 1.5 | 1.0 | 0.5 |     |     |     |     |      |     |     |     |     |  |  |  |  |
| <b>MODE 6:</b>  |     |     |     |     |     |     |     |     |     |     |      |     |     |     |     |  |  |  |  |
|                 | H-1 | H0  | H1  | H2  | --- |     |     | *   |     |     |      |     |     |     |     |  |  |  |  |
|                 | 4   | o   | 20  | 20  |     |     |     |     |     |     |      |     |     |     |     |  |  |  |  |
|                 |     |     | V1  | V2  | V3  | V4  | V5  |     |     |     |      |     |     |     |     |  |  |  |  |
|                 |     |     | 0.5 | 1.0 | 1.5 | 1.0 | 0.5 |     |     |     |      |     |     |     |     |  |  |  |  |
| <b>MODE 7:</b>  |     |     |     |     |     |     |     |     |     |     |      |     |     |     |     |  |  |  |  |
|                 | H-1 | H0  | H1  | H2  | --- |     |     | *   | --- |     |      | *   |     |     |     |  |  |  |  |
|                 | 4   | o   | 20  | 20  |     |     |     |     |     |     |      |     |     |     |     |  |  |  |  |
|                 |     |     | V1  | V2  | V3  | V4  | V5  | V6  | V7  |     |      |     |     |     |     |  |  |  |  |
|                 |     |     | 0.3 | 0.7 | 1.0 | 1.3 | 1.0 | 0.7 | 0.3 |     |      |     |     |     |     |  |  |  |  |
| <b>MODE 8:</b>  |     |     |     |     |     |     |     |     |     |     |      |     |     |     |     |  |  |  |  |
|                 | H-1 | H0  | H1  | H2  | H3  | --- |     |     | *   | --- |      |     | *   |     |     |  |  |  |  |
|                 | 4   | o   | 20  | 20  | 20  |     |     |     |     |     |      |     |     |     |     |  |  |  |  |
|                 |     |     | V1  | V2  | V3  | V4  | V5  | V6  | V7  | V8  |      |     |     |     |     |  |  |  |  |
|                 |     |     | 0.3 | 0.7 | 1.0 | 1.3 | 1.3 | 1.0 | 0.7 | 0.3 |      |     |     |     |     |  |  |  |  |
| <b>MODE 9:</b>  |     |     |     |     |     |     |     |     |     |     |      |     |     |     |     |  |  |  |  |
|                 | H-1 | H0  | H1  | H2  | H3  | H4  | H5  | --- |     |     | *    | --- |     |     | *   |  |  |  |  |
|                 | 4   | o   | 20  | 20  | 20  | 20  | 20  |     |     |     |      |     |     |     |     |  |  |  |  |
|                 |     |     | V1  | V2  | V3  | V4  | V5  | V6  | V7  | V8  | V9   | V10 | V11 | V12 | V13 |  |  |  |  |
|                 |     |     | 0.2 | 0.4 | 0.6 | 0.8 | 1.0 | 1.2 | 1.4 | 1.2 | 1.0  | 0.8 | 0.6 | 0.4 | 0.2 |  |  |  |  |
| <b>MODE 10:</b> |     |     |     |     |     |     |     |     |     |     |      |     |     |     |     |  |  |  |  |
| Virt. height:   | h0  | h'1 | h'2 | h'3 | h'4 | h'5 | h'6 | h'7 | h'8 | h'9 | h'10 | .   | .   | .   | .   |  |  |  |  |
| weight:         | o   | 1   | 1   | 1   | 1   | 1   | 1   | 1   | 1   | 1   | 1    | .   | .   | .   | .   |  |  |  |  |

heights above  $F_0$ , to ensure a smooth fit to previous segments. Real-height points below the origin have a reduced weight. Virtual-height weights are varied linearly from the ends of the current segment, and within a segment the weight employed is the lower of the values from the two linear variations. Thus for Modes 6 to 9 the weights are larger towards the centre and end of the profile segment to be calculated; this is desirable since a real-height interval is defined most accurately by virtual heights in this region (Titheridge, 1979). The weights are calculated and applied within the subroutine COEFIC, as described in Appendix D.1. Allowance is made for the dependence of the overall effective weight on the square of the mean size of the coefficients, and on the square of the multiplying factor, in determining factors to give the effective weights listed in Table 3.

#### 5.4 The Layer Peak

For each ionospheric layer, real heights are calculated directly only up to some frequency  $F_M$  which is less than the critical frequency  $F_C$ . Continuation of the profile, up to and across the layer peak, requires some assumption about the shape of the peak section. This is commonly taken to be parabolic. The last few calculated points can then be used to determine the effective scale height  $SH$ , the peak height  $HM$ , and (if it has not been scaled) the critical frequency  $F_C$ . This procedure is used in the simplified program SPOLAN (using a fit to calculated gradients, since these are defined most accurately).

The peak-calculation procedure in POLAN uses a somewhat different approach. It was designed specifically to incorporate the following features, for maximum accuracy and reliability.

- (a) Chapman theory (applicable to the E region) and diffusion calculations (for the F layer peak) show that the peaks have basically the shape of an  $\alpha$ -Chapman layer. For this layer, use of the parabolic approximation gives a consistent error of about -13% in the calculated scale heights (and -2km in  $HM$ , -0.01 MHz in  $F_C$ ). POLAN therefore uses a true Chapman-layer peak.
- (b) Virtual heights just before a peak generally show large group retardation. Thus they define primarily the gradient of the real-height profile. The calculated peak curvature should therefore depend only on the calculated gradients, at the scaled frequencies.
- (c) Peak parameters are obtained by a least-squares calculation using at least five profile points (when the data permit). Higher frequencies are given most weight, since they reflect the peak shape most closely. At the lower frequency end of the fitted range the weights decrease to zero. Results then depend only slightly on points further from the peak, and do not change abruptly with different scaling frequencies.
- (d) Critical frequencies can often be scaled from an ionogram with worthwhile accuracy. Provision is therefore made for the use of scaled ordinary or extraordinary-ray values. The scaled values are not assumed to be correct, but provide additional input to the least-squares calculation.
- (e) An estimate of the accuracy of the peak parameters is required.
- (f) As the amount of data available near the peak decreases, the calculated peak parameters must not become erratic or absurd but should tend smoothly towards some well-defined model.

Implementation of (a) to (f) involves formulation of the peak equations with plasma frequency  $F_N$  as a function of height  $h$  (instead of the usual  $h$  as a function of  $F_N$ ). This gives well-behaved functions which change slowly across the peak; it simplifies use of the Chapman-layer expression; and it enables critical frequency measurements to be incorporated directly into a least-squares solution. The basic equations involve only the scaled frequencies  $F_j$  and the gradients  $dh/dF_N$  at  $F_j$ . The least-squares solution gives  $\ln(F_C)$  and  $SH$ , and the standard errors in these quantities. The peak height  $HM$  is then obtained by fitting the calculated peak shape to the last few calculated heights.

The Chapman peak is expressed (exactly) as a parabolic peak plus a correcting term. The latter is determined by iteration, beginning with a model value  $SHA$  for the scale height. Only one iteration is used, so that the results still have some dependence on  $SHA$ . The correcting term disappears at the peak, and is large at lower frequencies. Thus when good data are available to within about 8% of the critical frequency, the final scale height  $SH$  is almost independent of  $SHA$ . When the highest scaled frequencies are further below  $F_C$ , the calculated  $SH$  is increasingly biased towards  $SHA$ . This fulfils condition (f) above; as the available data get too far from the peak to give a reliable estimate of peak curvature, the assumed curvature (defined by the scale height) tends to the model value.

Any scaled value of the ordinary-ray critical frequency is included in the least-squares solution, weighted so that the calculated FC will be shifted approximately half way to the scaled value. A scaled X-ray critical frequency FCX may also be given following the O-ray value. If the O-ray critical frequency is not scaled it must be replaced by zero (or the value of FCX must be negative), so that POLAN will recognise the next value as an X ray. Critical frequencies are identified by an associated virtual height of zero (or less than 30 km in absolute value). The first peak iteration provides a good estimate of the height, and hence the gyrofrequency, to use in converting FCX to the corresponding plasma frequency.

The model scale height currently used in POLAN is given by  $SHA = HN/4 - 20$  km, where HN is the last calculated real height. This gives reasonable mean values, and corresponds to the valley model of Section 7. If the calculated gradient at HN is not appreciably greater than the value at the centre of the fitted frequency range, the curvature is considered insufficient for accurate calculations and POLAN sets  $SH = SHA$ . This condition is signaled by printing SH negative in the output listing. FC is still obtained by fitting a Chapman peak to the profile gradients, but the use of a fixed scale height prevents unreasonable extrapolations.

A further check is made after the first least-squares solution. If the calculated peak height exceeds  $HN + SH$ , or the gradient is not increasing rapidly at HN, the solution is not iterated. This condition occurs when the highest scaled frequency is less than  $0.84FC$ . In this case calculation of SH (and FC) based entirely on the profile data is less reliable, so the final result is left with a heavier weight towards the model scale height SHA. With these precautions useful peak parameters are obtained under most conditions, and misleading results are avoided.

### 5.5 The Simplified Program SPOLAN

All procedures discussed in this report are incorporated in the computer program POLAN, described in Appendices D to F. A simpler program SPOLAN is also available, and is described in Appendix H. SPOLAN was developed to provide: (i) a shorter and faster alternative to POLAN, when extraordinary-ray calculations are not required; and (ii) a clearer demonstration of the basic logic used in POLAN.

By removing all extraordinary-ray calculations from SPOLAN the size and complexity of the program are considerably reduced. A parabolic peak-fitting procedure is used to obtain the scale height and the critical frequency from the gradients at the last two calculated points. This replaces the more accurate iterative Chapman peak calculation used by POLAN. SPOLAN also assumes a simple model valley between layers. Accuracy will be reduced at high latitudes since SPOLAN does not include the special procedure developed to counter integration errors at dip angles above  $70^\circ$  (Appendix B.3). A fixed order of integration (6-point Gaussian) is used instead of the 5- or 12-point options in POLAN; thus use of "MODE + 10" to increase the integration accuracy has no effect with SPOLAN. Finally SPOLAN uses a fixed value of gyrofrequency FB at all heights. This does not appreciably affect results for the ordinary ray provided that a suitable value of FB (corresponding to a height of about 150 to 200 km) is used.

Apart from the above points SPOLAN incorporates all the features of POLAN which are applicable to ordinary-ray analysis. From a user's viewpoint the programs POLAN and SPOLAN are identical when only ordinary-ray data are used. A SPOLAN user may therefore readily change to POLAN when increased accuracy at high dip angles, more accurate layer peaks, or more accurate start and valley calculations (using extraordinary rays) are desired.